

AC 2008-2725: DESIGN OF EXPERIMENTS APPROACH TO VERIFICATION AND UNCERTAINTY ESTIMATION OF SIMULATIONS BASED ON FINITE ELEMENT METHOD

Jeffrey Fong, National Institute of Standards and Technology

Jeffrey T. Fong was educated at the University of Hong Kong (B.Sc., Engineering, First Class Honors, 1955), Columbia University (M.S., Engineering Mechanics, 1961), and Stanford University (Ph.D., Applied Mechanics and Mathematics, 1966). From 1955 to 1963, he worked as an engineer in powerplant design and construction at Ebasco Services, Inc. in New York City, and earned a professional engineer's license to practice in the State of New York (P.E., 1962) and the British Commonwealth (A.M.I.C.E., London, U.K., 1968).

Since 1966, Dr. Fong has been a research engineer with the title of Physicist at the Mathematical and Computational Sciences Division of the National Institute of Standards and Technology (NIST) in Gaithersburg, Maryland. During his long association with NIST, he has published more than 80 technical papers and reports, and edited numerous conference proceedings in the areas of fatigue and fracture mechanics, nondestructive testing, mathematical and statistical modeling of inelastic behavior of materials, and engineering safety and failure analysis. In Jan. 2006, Dr. Fong was appointed Adjunct Visiting Research Professor of Structures and Statistics of the Department of Mechanical Engineering and Mechanics, Drexel University, Philadelphia, Pennsylvania, and was invited to teach graduate-level courses entitled "Finite Element Method with Uncertainty Analysis," and "Failure Analysis and Engineering Safety."

Elected Fellow of the American Society for Testing and Materials (ASTM) in 1982, Fellow of the American Society of Mechanical Engineers (ASME) in 1984, and an ASME National Distinguished Lecturer from 1988 to 1992, Dr. Fong received in 1993 one of ASME's highest awards, the Pressure Vessel and Piping Medal.

James Filliben, National Institute of Standards and Technology

James J. Filliben is currently Leader of the Statistical Modeling and Analysis Group in the Statistical Engineering Division of the Information Technology Laboratory at the National Institute of Standards and Technology (NIST), Gaithersburg, Maryland.

He earned his BA (1965) in Mathematics from LaSalle College, and PhD (1969) in Statistics from Princeton University. He joined the technical staff of NIST in 1969, and has more than 50 papers in refereed journals and 200 talks and short courses to his credit. In 2003, he became a Fellow of the American Statistical Association.

Alan Heckert, National Institute of Standards and Technology

Alan Heckert earned his B.S. degree in mathematics at the Frostburg State University in 1978, and his M.S. in mathematics/statistics at the Clemson University in 1980. He worked at the Census Bureau from 1981 to 1985, and has been a Computer Specialist in the Statistical Engineering Division of the National Institute of Standards and Technology, Gaithersburg, Maryland, since 1985.

Alan Heckert's technical areas of interest are statistical graphics and statistical computing. He is a member of the American Statistical Association and was honored by the U.S. Department of Commerce (DoC) with the award of a DoC Silver Medal in 2003.

Roland deWit, National Institute of Standards and Technology

Roland deWit was educated at the Ohio University, Athens, Ohio (B.S., Liberal Arts with major in Mathematics, 1953), and University of Illinois, Urbana, Illinois (Ph.D., Physics, 1959). His professional experience has been with the Physics Department, University of Illinois (1959,

Research Associate), Department of Mineral Technology, University of California, Berkeley, CA (1959-60, Assistant Research Physicist), and the Metallurgy Division of the Materials Science and Engineering Laboratory, NIST, Gaithersburg, MD (1960-1998, Physicist (Solid State)). Since 1998, he has been a Guest Researcher at NIST and a Consultant based in Potomac, Maryland.

Dr. deWit has published more than 50 technical papers in four major areas: Dislocation Theory (contributed to the development of a continuum theory of dislocations and disclinations); Fracture Mechanics (participated in the testing and analysis of the dynamic fracture of pressure vessel steels and the tearing fracture of aluminum sheets with multi-state damage); Mechanical Properties (contributed to the theory of overall elastic properties of polycrystals); and Finite Element Analysis (developed simulation models for large plastic deformations). He was co-editor of the conference proceedings "Fundamental Aspects of Dislocation Theory" and the "Fourth International Congress for Stereology," and the English translation of the Russian book "Mechanics of Brittle Fracture" by A. Cherepanov. A number of Dr. deWit's papers have also been translated into Russian and published under the title "Continuum Theory of Disclinations."

Design of Experiments Approach to Verification and Uncertainty Estimation of Simulations based on Finite Element Method (*)

Abstract

A fundamental mathematical modeling and computational tool in engineering and applied sciences is the finite element method (FEM). The formulation of every such problem begins with the building of a mathematical model with carefully chosen simplifying assumptions that allow an engineer or scientist to obtain an approximate FEM-based solution without sacrificing the essential features of the physics of the problem. Consequently, one needs to deal with many types of uncertainty inherent in such an approximate solution process. Using a public-domain statistical analysis software package named DATAPLOT¹, we present a metrological approach to the verification and uncertainty estimation of FEM-based simulations by treating each simulation as a "virtual experiment." Similar to a physical experiment, the uncertainty of a virtual experiment is addressed by accounting for its physical (modeling), mathematical (discretization), and computational (implementation) errors through the use of a rigorous statistical method known as the design of experiments (DOE). An introduction of the methodology is presented in the form of five specific topics: (a) the fundamentals of DOE, (b) the assumptions of model building, (c) setting objectives for an experiment, (d) selecting process input variables (factors) and output responses, and (e) weighing the objectives of the virtual experiment versus the number of factors identified in order to arrive at a choice of an experimental design. The method is then specialized for FEM applications by choosing a specific objective and a subclass of experimental designs known as the fractional factorial design. Two examples of this FEM-specific approach are included: (1) The free vibration of an isotropic elastic cantilever beam with a known theoretical solution, and (2) The calculation of the first resonance frequency of the elastic bending of a single-crystal silicon cantilever beam without known solutions. In each example, the FEM-simulated result is accompanied by a prediction 95% confidence interval. Significance and limitations of this metrological approach to advancing FEM as a precision simulation tool for improving engineering design appear at the end of this paper.

(*) Contribution of the National Institute of Standards & Technology. Not subject to copyright.

Introduction

A fundamental mathematical modeling and computational tool in science and engineering today is the finite element method (see, e.g., Hughes², and Zienkiewicz³). The method, abbrev. FEM, originated from aerospace applications in the 1960s where large scale fuselage, wings, tail assembly, and engines needed a new tool to relate their complex geometry, materials properties, loadings and uncertainties to performance within a reasonable margin of safety. The method was adopted by the nuclear power industry in the '70s and the automobile manufacturers in the '80s to improve design and ensure safety of critical components and systems. Since then, a large number of proprietary, commercially-available^{4,5,6}, and public domain⁷ FEM software packages has appeared with applications not only in all branches of engineering but also as a modeling and simulation tool in basic and applied sciences such as biology^{8,9}, biomechanics^{10,11}, microelectromechanical systems (MEMS)¹², and nanotechnology¹³.

The problem with any given FEM software package is that it seldom delivers simulations with an estimate of uncertainty due to variability in geometry, material properties, loadings, and software implementation. For engineering applications, the lack of uncertainty estimates is generally accepted since decisions are made with judgment and code-prescribed safety factors. For advanced engineering and scientific research, where input parameters are not well characterized and the fundamental governing equations are not even known in some cases and thus the objects of investigation, such lack in FEM simulations falls short for making them credible prior to a process of verification for mathematical and computational correctness and validation against physical reality.

During the last two decades, advances in model and simulation verification and validation (abbrev. V&V) dealing with (a) uncertain input and uncertainty in modeling (see, e.g., Ayyub¹⁴, 1998; Lord and Wright¹⁵, 2003; and Hlavacek¹⁶, 2004), (b) V&V (see, e.g., Oberkampf¹⁷, 1994; Roache¹⁸, 1998; Oberkampf, Trucano, and Hirsch¹⁹, 2002; Babuska and Oden²⁰, 2004; and Fong, et al²¹, 2005), and (c) validation in the context of metrology (see, e.g., Butler, et al²², 1999; and Fong, et al²³, 2006), have appeared in the literature. Government agencies and professional societies have also added their concern and made major contributions in the form of directives²⁴, guides^{25,26,27}, and reviews²⁸. Significant advances in V&V of FEM simulations have also been reported (see, e.g., Haldar, Guran, and Ayyub²⁹, 1997; Haldar and Mahadevan³⁰, 2000; Yang, et al³¹, 2002; and Fong, et al³²).

Unfortunately, the problem is hard and progress has been slow for two reasons, one being obvious and the other not so obvious from a technical standpoint. The lack of adequate funding is the obvious one, but, surprisingly, the lack of a statistical perspective is the other as noted below in a 2002 review of the state of the art of V&V by Oberkampf, Trucano, and Hirsch¹⁹:

"... In the United States, the Defense Modeling and Simulation Office (DMSO) of the Department of Defense (DOD) has been the leader in the development of fundamental concepts and terminology for V&V.

"... Of the work conducted by DMSO^{24,25}, Cohen²⁸ observed: 'Given the critical importance of model validation ... , it is surprising that the constituent parts are not provided in the DOD directive²⁴ concerning validation. *A statistical perspective is almost entirely missing in these directives.*' We believe this observation properly reflects the state of the art in V&V, not just the directives of DMSO. That is, the state of the art has not developed to the place where one can clearly point out all of the actual methods, procedures, and process steps that must be undertaken for V&V." [Italics added by the authors of this paper.]

The purpose of this paper is, therefore, two fold: (1) To introduce a statistical perspective to the general problem of V&V with a metrological approach, and (2) to specialize this approach to a subclass of the V&V problem, namely, the FEM-based simulations, with a goal of estimating a prediction 95% confidence interval for any response variable of a finite element model. This metrology-based approach consists of two old ideas and two new tools as shown below:

- Idea No. 1. Each FEM-based simulation is treated as a "virtual experiment." Since the expression of uncertainty in a physical experiment is well known in the metrology literature^{33,34}, where the result of a measurement is considered complete only when accompanied by a quantitative statement of its uncertainty, we extend this idea and its associated error definitions to all FEM-based simulations.
- Idea No. 2 As a virtual experiment, every FEM-based simulation is required to have an associated experimental design, with which a goal of estimating a prediction 95% confidence interval for any response variable is attainable. Again, the statistical theory of design of experiments, abbrev. DOE, has been known for a long time (see, e.g., Natrella³⁵, 1963; John³⁶, 1971; Box, Hunter and Hunter³⁷, 1978; and Montgomery³⁸, 2000).
- Tool No. 1 A public-domain electronic handbook on statistical methods³⁹, that first appeared in 2003 with a clear exposition on DOE, and numerous examples and case studies for introductory and in-depth learning. Based on that handbook, we present a brief summary of the basic ideas of DOE before we use the second tool to estimate the confidence interval.
- Tool No. 2 A public-domain statistical software package named DATAPLOT¹.

To present this new approach, we divide the paper into four parts. Part I is a statement of the problem and a rationale of our solution approach. In Part II, we introduce DOE through a brief exposition based on Croarkin, et al³⁹ by discussing each of the following five topics:

- Topic A. Fundamentals of DOE.
 Topic B. Assumptions of model building.
 Topic C. Setting objectives for an experiment.
 Topic D. Selecting process input variables (factors) and output responses.
 Topic E. Weighing objectives of the experiment versus the number of factors in order to arrive at a choice of an appropriate experimental design.

In Part III, we choose, for FEM applications, a specific objective and a subclass of experimental designs known as the fractional factorial design for two-level experiments (see, e.g., Box, Hunter, and Hunter³⁷, pp. 374-433). Finally, in Part IV, we give two examples to illustrate this DOE approach: (1) The FEM simulation of the free vibration of an isotropic elastic cantilever beam, of which a theoretical solution is known^{40,41}. (2) The calculation of the first resonance frequency of the elastic bending of a single-crystal silicon cantilever beam using FEM, for which no known solution exists³². Significance and limitations of this approach to verification and uncertainty estimation of FEM-based simulations are discussed at the end of this paper.

Part I. Nature of the Problem and the Solution Approach

To characterize the nature of the problem, we examine three major classes of errors, whenever a user of a FEM software package attempts to formulate a model and obtain a computer-generated

numerical simulation. The three classes are: physical (modeling), mathematical (discretization), and computational (implementation), as amplified below:

Class A. Physical (modeling) errors due to the *inexactness* of input parameters, and, in some cases, *unknown* governing equations.

This class of errors reflects a fundamental difficulty in all branches of continuum physics, where the number of response variables (or degrees of freedom) exceeds the number of governing equations given by the laws of conservation of linear and angular momenta and the first and second laws of thermodynamics. To complete a well-posed mathematical model, the missing equations are postulated by engineers or scientists with coefficients based on experimental evidence, and can be broken down into three categories: (a) constitutive laws, linear or nonlinear, of material properties that relate one set of response variables (e.g., displacements) to another set (e.g., stresses), (b) atomic and molecular interaction laws that relate motion variables to forces, and (c) friction coefficients that relate interfacial motion to tangential and normal forces. Any attempt to obtain a numerical solution by FEM with a less-than-fully-understood set of governing equations and boundary conditions is subject to errors only a FEM user is intimately familiar with.

Class B. Mathematical (discretization) errors due to subdivisions in space, choice of steps in time, order of approximations, and iterative schemes for nonlinear problems.

All FEM simulations begin with a discretization scheme, or the so-called mesh design, which is user-dependent. For a fixed mesh design, the simulation delivers an approximate solution with a discretization error *on top of the Class A (Physical) error* due to an assumed governing system of equations, a set of input parameters such as the geometrical data, the material property and physical constants, and the discretization of the initial and boundary conditions. In theory, as the mesh design becomes progressively more refined, the results should converge to a "correct" solution. In practice, during a process (again user dependent) of grid convergence through mesh refinement, the finite precision of a real number in a computer sets a limit, beyond which the round-off error overwhelms the discretization error. For different mesh designs and, in case of nonlinear problems, different iterative schemes, the paths of grid convergence for FEM simulations of a given problem generally do not lead to identical results.

It is worth mentioning that, by definition, any measure of Class B error is equal to or greater than Class A error, because no computation can proceed without first formulating a discretized model from a continuum one with a built-in Class A error. However, most FEM users ignore Class

A error or assume it to be zero for a fixed model, and proceed to make Class B error estimates using numerical analysis techniques (see, e.g., Zienkiewicz and Taylor³ [Chap. 14, pp. 365-400]). For convenience, we shall adopt this convention and make estimates of Class B error for a fixed model assuming Class A error associated with that model to be zero.

Class B*. Mathematical (geometric nonlinearity) errors due to large deformation.

For the sake of completeness, it is important to include another class of errors that is geometric in nature. In modeling physical experiments in biotechnology, chemical physics, fluid-structural interactions, and structural instability (buckling), where the motion is generally large and a linearized model is no longer adequate, the problem becomes nonlinear, and the traditional representation of a particle in either Lagrangian or Euler formulation needs to be augmented by very costly iterative schemes. FEM simulations using different iterative schemes for different Lagrangian/Euler formulation yield non-identical and sometimes non-convergent results. However, for this expository paper on DOE with examples of very small displacements, we will ignore this class for brevity.

Class C. Computational (implementation) errors due to the *non-uniqueness* of FEM software system engineering.

As computing power increased, so did the complexity of the FEM software systems, which today often involve millions of lines of code. Those complex codes, developed over many years by large teams, routinely deliver simulations without a global "guarantee" of correctness, and the users must devote considerable resources to plan and conduct *ad-hoc* numerical experiments before using the software with confidence. The fact that lessons learned during those *ad-hoc* experiments are seldom documented and calibrated with benchmarks gives rise to a trustworthy issue, i.e., different FEM software gives different results of simulations for the same mesh design and mathematical model of a specific physical reality.

Generally speaking, when the material property constitutive equations of a mathematical model are postulated for lack of sufficient experimental evidence such as the thermal-mechanical time-dependent deformation of a nuclear reactor fuel rod, the Class A (physical) error estimates lead to uncertainties of a much larger magnitude than either B or C. We will illustrate this with a preview of our Example 1 in this section and later in Part IV a proof of that assertion.

As stated earlier, Example 1 is the FEM simulation of the free vibration of an isotropic elastic cantilever beam, of which a theoretical solution exists in the literature^{40,41}. As shown in Fig. 1, the formula for the first resonance frequency, Freq-1, of an isotropic elastic cantilever beam of length L , when specialized to a rectangular beam cross-section of thickness t , is given by the following simple formula:

$$(\text{Freq-1})_{\text{Isotropic}} = \frac{1}{2\pi} (1.875)^2 \sqrt{\frac{E}{12\rho}} \frac{t}{L^2} = 0.161522 \sqrt{\frac{E}{\rho}} \frac{t}{L^2}. \quad (1)$$

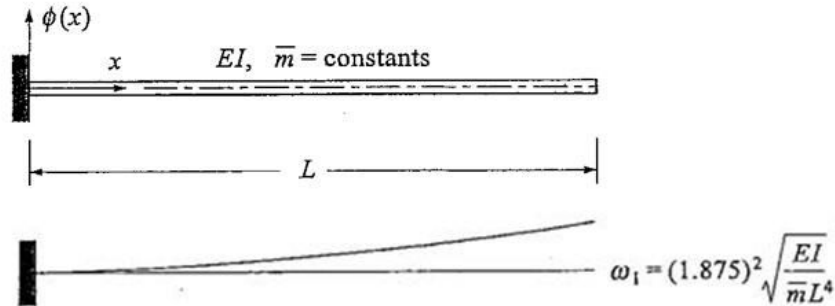


Fig. 1. Simple beam-vibration analysis: (Top) Basic properties of simple beam, i.e., Young’s modulus, E , moment of inertia, I , mass per unit length, \bar{m} , and length of the beam, L , and (bottom) the theoretical solution for the resonance frequency of the first vibration mode. After Clough and Penzien⁴¹, p. 380, Fig. E18-1. Note: If we assume a beam with a rectangular cross section of width w , and thickness t , and if the mass density per unit volume is given by ρ , the term I/\bar{m} becomes $t^2/(12\rho)$, which is independent of the width w .

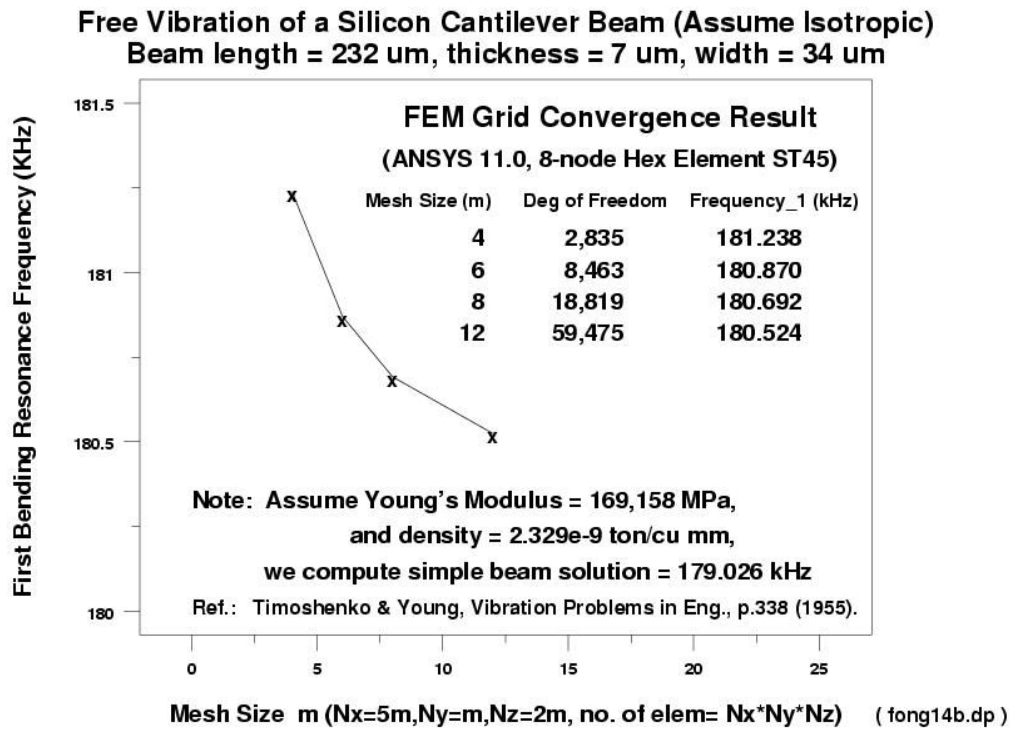


Fig. 2. A plot of the first bending resonance frequency (kHz) versus Mesh Size, m , in a FEM (ANSYS v.11.0) simulation of the free vibration of an isotropic elastic cantilever beam.

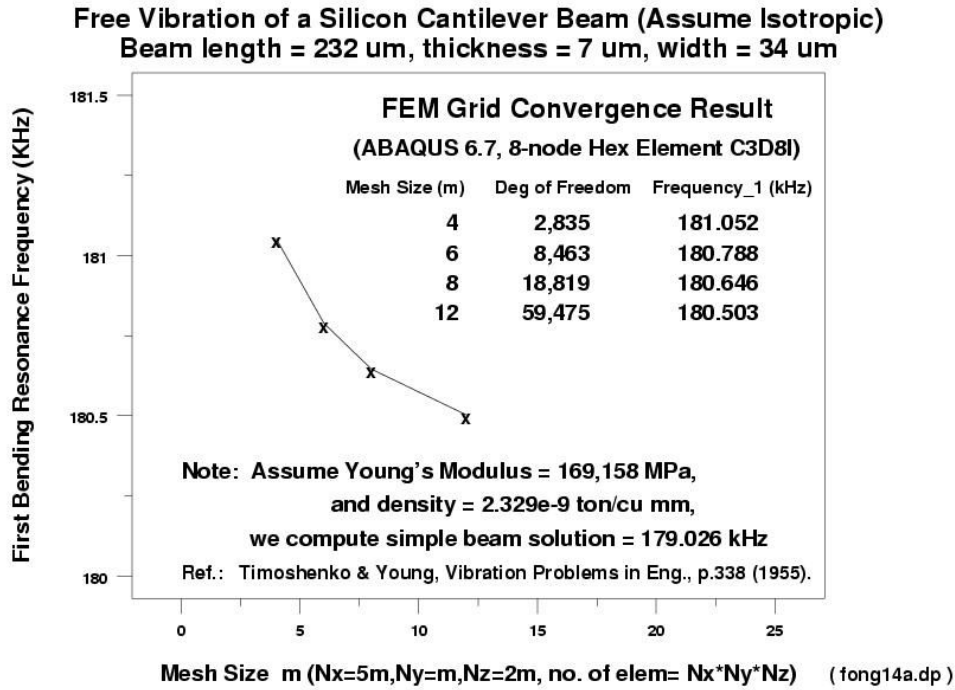


Fig. 3. A plot of the first bending resonance frequency (kHz) versus Mesh Size, m , in a FEM (ABAQUS v.6.7) simulation of the free vibration of an isotropic elastic cantilever beam.

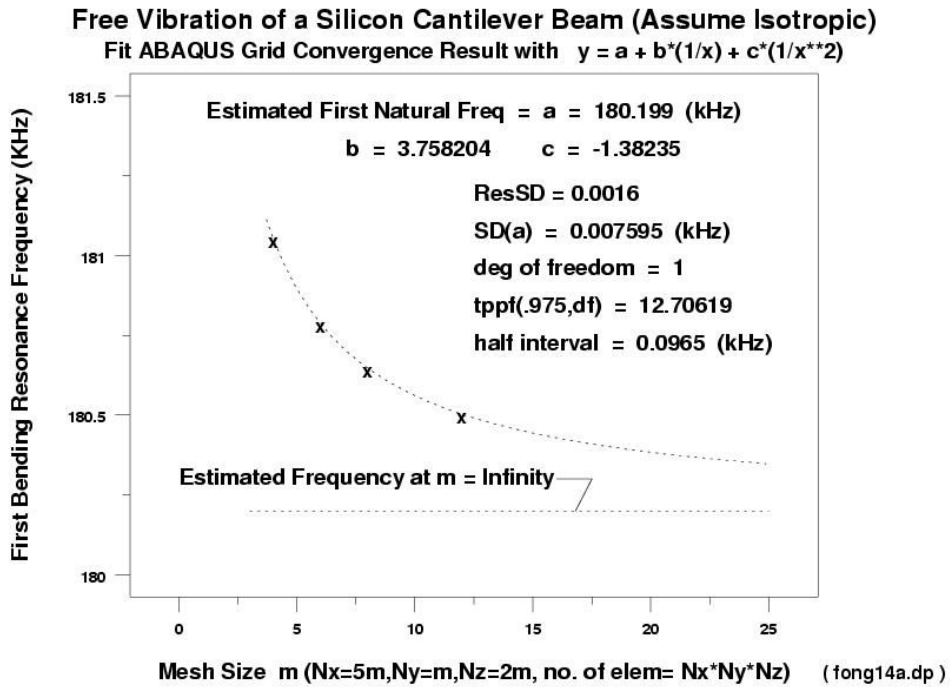


Fig. 4. A plot of the least square fit of the four-mesh ABAQUS result using an inverse quadratic model, $y = a + b/x + c/x^2$. Note that the frequency at $m = \text{infinity}$ is given by the parameter a .

**Free Vibration of a Silicon Cantilever Beam (Assume Isotropic)
Approach-1: Compare Grid Convergence Result with Theoretical**

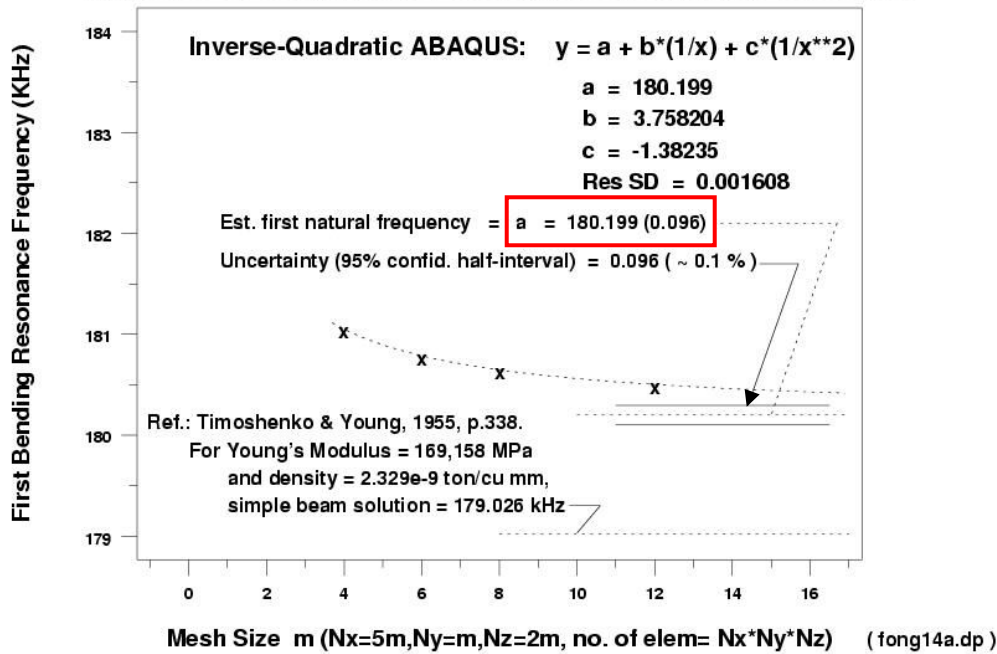


Fig. 5. From a re-plot of Fig. 4, we show that the estimated frequency from a least square fit of the model fails to match the theoretical solution. Note that in the red box, we represent the uncertainty of an estimated mean by the 95% half-interval in brackets following the mean.

We now present results of two FEM simulations, one using ANSYS v.11.0 (Fig. 2), and the other, ABAQUS (Fig. 3). We used the standard 8-node hexahedron (brick) element for a 4-mesh grid convergence test, and found both results quite satisfactory but numerically different. This illustrates the existence of Class C error due to software implementation. In Fig. 4, we show the result of a least square fit of an inverse quadratic model, $y = a + b/x + c/x^2$, for the 4-mesh ABAQUS simulation data, where the parameter, a , is the estimated frequency as mesh size approaches infinity (corresponding to a change from a discrete to a continuum body). In Fig. 5, we replotted the results of Fig. 4 to show that the asymptotic value of the FEM-simulated result failed to match the theoretical solution. This illustrates the existence of Class B error due to a combination of mesh design choice and finite machine round-off. In Part IV, Example 1, we will complete the investigation by quantifying the errors of all three classes defined earlier.

The definition of three classes of FEM simulation errors and the preview of Example 1 lead us to a statement of our solution approach. Basically, our ideas No. 1 (virtual experiment) and No. 2 (each simulation having a DOE) provide a basis to address errors of all three classes, because in a statistical design of experiments, we are free to identify as many input variables (factors) and output responses as we wish. To address Class A errors, we will identify as many *inexact* input parameters as "appropriate", so long as we have a "good" idea of their variability. To address Class B errors, we will take into consideration the mesh design, time increment, and mesh refinement for grid convergence when we list additional factors. To address Class C errors, we will consider different FEM packages and their element types also as factors in an experimental

design. We will, of course, end up with a large number of factors, but by using fractional factorial design of two-level experiments, we can reduce the number of computer runs to a manageable size in order to estimate uncertainty as a prediction 95% confidence interval.

Part II. Topic A: Fundamentals of DOE (see Croarkin, et al³⁹, Chap. 5, Sect. 5.1, pp. 9-20)

In an experiment, we change one or more process variables (factors) in order to observe the effect the changes have on one or more response variables. DOE is an efficient procedure for planning experiments so that the data obtained can be analyzed to yield valid and objective conclusions.

DOE begins with determining the *objectives* of an experiment and selecting the *process factors* for the study. An Experimental Design is the laying out of a detailed experimental plan in advance of doing the experiment. Well chosen experimental designs maximize the amount of "information" that can be obtained for a given amount of experimental effort.

The statistical theory underlying DOE begins with the concept of *process models*. A process model of the 'black box' type is formulated with several discrete or continuous input *factors* that can be controlled, and one or more measured output *responses*. The output responses are assumed continuous. Real or virtual experimental data are used to derive an empirical (approximate) model linking the outputs and inputs. These empirical models generally contain *first-order (linear) and second-order (quadratic) terms*.

The most common empirical models fit to the experimental data take either a *first- or second-order* form. A first-order model with three factors, X_1 , X_2 and X_3 , can be written as

$$Y = \beta_0 + \beta_1 X_1 + \beta_2 X_2 + \beta_3 X_3 + \beta_{12} X_1 X_2 + \beta_{13} X_1 X_3 + \beta_{23} X_2 X_3 + \text{errors} \quad (2)$$

Here, Y is the response for given levels of the main effects X_1 , X_2 and X_3 , and the $X_1 X_2$, $X_1 X_3$, $X_2 X_3$ terms are included to account for a possible interaction effect between X_1 and X_2 , X_1 and X_3 , X_2 and X_3 , respectively. The constant β_0 is the response of Y when both main effects are 0. In Example 1, we use a linear model with three factors and one response variable, and a complete representation of that model contains just 8 terms on the right hand side of eq. (2), i.e., a constant term, three main effects terms, three two-way interaction terms and one three-way interaction term. In Example 2, we use a linear model with five factors and one response variable, and total number of terms on the right hand side of eq. (2) is 2^5 , or 32.

A second-order (quadratic) model (typically used in response surface DOE's with suspected curvature⁴²) does not include the three-way interaction term but adds three more terms to the first-order model (2), namely

$$\beta_{11} X_1^2 + \beta_{22} X_2^2 + \beta_{33} X_3^2.$$

Note: Clearly, a full model could include many cross-product (or interaction) terms involving squared X 's. However, in general these terms are not needed and most DOE software defaults to leaving them out of the model.

This concludes Section 5.1.1 of Croarkin, et al³⁹ on "What is experimental design?" The reader is invited to read Croarkin, et al³⁹ for the two follow-up sections, namely, Section 5.1.2 on "What are the uses of DOE?" and Section 5.1.3 on "What are the steps of DOE?"

Topic B: Assumptions of model building (see Croarkin, et al³⁹, Chap. 5, Sect. 5.2, pp. 21-34)

In all model building we make assumptions, and we also require certain conditions to be approximately met for purposes of estimation. In Section 5.2 of Croarkin, et al³⁹, we look at some of the engineering and mathematical assumptions we typically make. These are:

- (a) Are the measurement systems capable for all of your responses?
- (b) Is your process stable?
- (c) Are your responses likely to be approximated well by simple polynomial models?
- (d) Are the residuals (the difference between the model predictions and the actual observations) well behaved?

Again, the reader is invited to read Croarkin, et al³⁹ for more on this topic.

Topic C: Setting objectives for an experiment (see Croarkin, et al³⁹, Chap. 5, Sect. 5.3.1)

The objectives of an experiment are best determined by a team discussion. All of the objectives should be written down, even the "unspoken" ones. There are four broad categories of experimental designs, with various objectives for each. These are:

Table 1. 4 Categories of Experimental Designs and 8 Objectives for an Experiment

<u>Design</u>	<u>Objective</u>
Comparative designs	To choose between alternatives, with narrow scope, suitable for an initial comparison.
	To choose between alternatives, with broad scope, suitable for a confirmatory comparison.
Screening designs	To identify which factors/effects are important.
Response Surface designs	To maximize or minimize a response.
	To reduce variation by locating a region where it is easier to manage.
	To make a process robust (note: this objective may often be accomplished with screening designs rather than with response surface designs).
Regression modeling	To estimate a precise model, quantifying the dependence of response variable(s) on process inputs.

Topic D: Selecting variables (factors and responses) (see Ref. 39, Sect. 5.3.2, pp. 39-41)

Process variables include both inputs (factors) and outputs (responses). The selection of these variables is best done as a team effort. The team should

- (a) Include all important factors (based on engineering judgment).
- (b) Be bold, but not foolish, in choosing the low and high factor levels.
- (c) Check the factor settings for impractical or impossible combinations, such as very low pressure and very high gas flows.
- (d) Include all relevant responses.
- (e) Avoid using only responses that combine two or more measurements of the process. For example, if interested in selectivity (the ratio of two etch rates), measure both rates, not just the ratio.

We have to choose the range of the settings for input factors, and it is wise to give this some thought beforehand rather than just try extreme values. In some cases, extreme values will give runs that are not feasible; in other cases, extreme ranges might move one out of a smooth area of the response surface into some jagged region, or close to an asymptote.

The most popular experimental designs are *two-level designs*. Why only two levels? There are a number of good reasons why two is the most common choice amongst engineers; one reason is that it is ideal for screening designs, simple and economical; it also gives most of the information required to go to a multilevel response surface experiment if one is needed.

The standard layout for a 2-level design uses +1 and -1 notation to denote the "high level" and the "low level" respectively, for each factor. For example, the matrix below

	Factor 1 (X1)	Factor 2 (X2)
Trial 1	-1	-1
Trial 2	+1	-1
Trial 3	-1	+1
Trial 4	+1	+1

describes an experiment in which 4 trials (or runs) were conducted with each factor set to high or low during a run according to whether the matrix had a +1 or -1 set for the factor during that trial. If the experiment had more than 2 factors, there would be an additional column in the matrix for each additional factor. Note: An alternative convention is to shorten the matrix notation for a two-level design by just recording the plus and minus signs, leaving out the "1's".

To introduce the concept of a center point, we include in this topic a graphical representation of a two-level, full factorial design for three factors, namely, the 2^3 design (see Fig. 6). This implies

eight runs (not counting replications or center point runs). The arrows show the direction of increase of the factors. The numbers '1' through '8' at the corners of the design box reference the "Standard Order" of runs (also referred to as the "Yates Order").

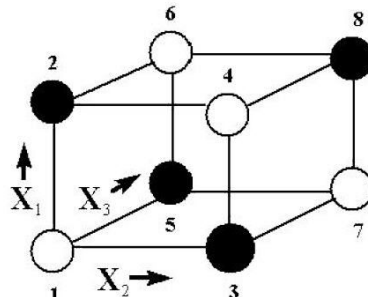


Fig. 6. A 2^3 two-level, full factorial design; factors X_1 , X_2 , X_3 .

As mentioned earlier, we adopt the convention of +1 and -1 for the factor settings of a two-level design. When we include a center point during the experiment, we mean a point located in the middle of the design cube, and the convention is to denote a center point by the value "0". For a more detailed exposition of the two-level design, the reader is invited to read the remaining pages of Ref. 39, Chap. 5, Section 5.3.2, pp. 39-41.

Topic E: Weighing objectives vs. number of factors (see Ref. 39, Sect. 5.3.3, pp. 42-44)

The choice of an experimental design depends on the objectives of the experiment and the number of factors to be investigated. Ref. 39, Section 5.3.3, pp. 42-44, gives a detailed discussion of this very important topic, including a concise table of guidelines when one weighs the objectives versus the number of factors (see Table 2):

Table 2. Design Selection Guideline³⁹

<u>Number of Factors</u>	<u>Comparative Objective</u>	<u>Screening Objective</u>	<u>Response Surface Objective</u>
1	1-factor completely randomized design	—	—
2 - 4	Randomized block design	Full or fractional factorial	Central composite or Box-Behnken
5 or more	Randomized block design	Fractional factorial or Plackett-Burman	Screen first to reduce number of factors

Table 2 refers to a number of designs that are well-known as a subset of a much larger set of designs available in the literature as enumerated below:

Design Type 1.	Completely randomized designs.
Design Type 2.	Randomized block designs, which include Latin squares, Graeco-Latin squares, and Hyper-Graeco-Latin squares.
Design Type 3.	Full factorial designs, which include two-level full factorial designs, three-level full factorial designs, and a discussion of the blocking of full factorial designs.
Design Type 4.	Fractional factorial designs.
Design Type 5.	Plackett-Burman designs.
Design Type 6.	Response surface (second-order) designs, which include central composite designs, Box-Behnken designs, and blocking a response surface design.
Design Type 7.	Adding center points.
Design Type 8.	Three-level, mixed level and fractional factorial designs.
Design Type 9.	D-Optimal designs.
Design Type 10.	Taguchi designs.
Design Type 11.	John's $\frac{3}{4}$ fractional factorial designs.
Design Type 12.	Small composite designs.
Design Type 13.	Mixture designs, which include simplex-lattice designs, simplex-centroid designs, and constrained mixture designs.

We refer the reader to Ref. 39, Chapter 5, for a detailed study of those types. It is a good idea to choose a design that requires somewhat fewer runs than the budget permits, so that center point runs can be added to check for curvature in a 2-level screening design and backup resources are available to redo runs that have processing mishaps.

Part III. Application of a DOE Approach to FEM Simulations.

For an application of the DOE approach to FEM simulations, we choose the screening objective and a two-level fractional factorial design that is applicable to any number of factors larger than 1 (see Table 2). The availability of (a) a public-domain statistical analysis software package named DATAPLOT¹, and (b) the documentation of an exploratory data analysis (EDA) approach of DATAPLOT for analyzing the data in 10 steps from a designed experiment (see Croarkin, et

al³⁹, Chap. 5, Section 5.5.9, pp. 313-412), made it possible for us to implement a specific application of the proposed DOE approach to FEM-based simulations.

Let us introduce the so-called EDA approach of DATAPLOT to a screening problem in experimental design and its 10-step algorithm. In general, there are two characteristics of a screening problem: (a) There are many factors to consider. (b) Each of these factors may be either continuous or discrete. The desired output from the analysis of a screening problem is:

1. A ranked list (by order of importance) of factors.
2. The best settings for each of the factors.
3. A good model.
4. Insight.

The essentials of the screen problem are:

1. There are k factors with n observations.
2. The generic model is

$$Y = f(X_1, X_2, \dots, X_k) \quad (3)$$

In particular, the EDA approach implemented in DATAPLOT is applied to 2^k full factorial and 2^{k-p} fractional factorial designs. Let us introduce a 10-step EDA process for analyzing the data from 2^k full factorial and 2^{k-p} fractional factorial designs as follows: (Note: For consistency with Ref. [39] in which DOE was replaced by DEX as an abbreviation for design of experiments, we list below the titles of each step with a joint abbreviation, DOE/DEX .)

- | | |
|----------|---|
| Step 1. | Ordered data plot. |
| Step 2. | DOE/DEX scatter plot. |
| Step 3. | DOE/DEX mean plot. |
| Step 4. | Interaction effects matrix plot. |
| Step 5. | Block plot. |
| Step 6. | DOE/DEX Youden plot. |
| Step 7. | Effects plot. |
| Step 8. | Half-normal probability plot. |
| Step 9. | Cumulative residual standard deviation plot. |
| Step 10. | DOE/DEX contour plot of two dominant factors. |

Each of these plots will be presented with the following format:

1. Purpose of the plot.
2. Output of the plot.
3. Definition of the plot.
4. Motivation for the plot.
5. An example of the plot.
6. A discussion of how to interpret the plot.
7. Conclusions we can draw from the plot for the example data.

Part IV. Two Examples

Example 1. Free Vibration of an Isotropic Elastic Cantilever Beam

For a free vibration problem of an isotropic elastic cantilever beam, let us denote the length of the beam by L . Assuming the beam has a rectangular cross-section of width w , and thickness t , we denote the two material property constants of the beam by E , its Young's modulus, and ν , Poisson's ratio. Let the density of the beam be denoted by ρ . As shown in Part I, eq. (1), it is known^{40,41} that the first bending resonance frequency of such beam depends only on four of its six parameters, namely, L , t , E , and ρ .

Motivated by an application in atomic force microscopy where a cantilever beam is made of silicon, and adopting the SI units of mm, ton, s, N, and MPa, we assign the values of the four parameters as follows: $L = 0.232$, $t = 0.007$, $E = 169,158$, and $\rho = 2.329\text{e-}09$. Let Y be the response variable of the problem, i.e., the resonance frequency of the first bending mode of the free vibration of the cantilever beam, we apply eq. (1) to compute that $Y = 179.026$ kHz.

For this example of FEM simulations, we shall use two commercially-available packages, namely, ABAQUS⁴, version 6.7, and ANSYS⁵, version 11.0. For each package, we shall use an 8-node brick (hexahedron) as the basic element. Considering a Cartesian coordinate system where the length, thickness, and width of the beam are oriented in the x , y , and z directions, respectively, and assuming the beam is uniformly subdivided into brick elements, we define N_x , N_y , N_z as the number of subdivisions in x , y , and z directions, respectively. Let m be a positive integer that denotes the size of a mesh design, and for this example, we shall adopt a specific design such that $N_x = 5m$, $N_y = m$, and $N_z = 2m$. Thus the total number of elements for this class of design is $10 m^3$. As m increases, the mesh is progressively refined such that the discretized finite element model approaches a continuum as m approaches infinity. As shown in Table 3 showing the FEM results presented earlier in Part I, Figs. 2 through 5, the frequency estimated from a 4-mesh grid convergence technique fails to match the theoretical solution.

Table 3. 4-Mesh Simulation Results and Grid Convergence Estimates of FEM Uncertainty

Mesh size	No. of elements	No. of nodes	Degrees of freedom	Y (kHz) (ABAQUS)	Y (kHz) (ANSYS)
4	640	945	2,835	181.052	181.238
6	2,160	2,821	8,463	180.788	180.870
8	5,120	6,273	18,819	180.646	180.692
12	17,280	19,825	59,475	180.503	180.524
<i>infinity</i> (via a least square fit, Figs. 4 and 5)	..			180.199 (0.096)	180.201 (0.081)

In short, this example illustrates that, because of additional errors such as round-off and matrix solver routines that have not been accounted for, there is always the difficulty of using a grid convergence technique to progressively refine the mesh of a discretized model to the "correct" limit of a continuum. At best, we use a least square approximation technique in this exercise to estimate the so-called Class B errors due to spatial discretization. For ABAQUS simulation, that

Example 1 - Continued

error is $180.199 - 179.026 = 1.173$ kHz, or about 0.66 %, and the same is true for the ANSYS simulation, even though the two simulations do not seem to be identical. Without knowing a theoretical solution, the only uncertainty we can calculate using the grid convergence method is the prediction 95% confidence half-interval, which is 0.096 kHz or 0.081 kHz, for ABAQUS or ANSYS simulations, respectively. This ends our investigation for Class B error (mathematical).

We now turn our attention to a method to address both Class A and Class C errors. For this, we introduce our new approach by using the method of DOE. Our first step is to construct a table of factors and their two-level variabilities. As shown in Fig. 6, a 3-factor 2-level DOE needs 8 runs for a full-factorial, and only 4 runs for a half-factorial design. We plan to use both designs in this example to gain some valuable insight into the difference between those two designs. The center point around which we choose to conduct the 8-run and 4-run experiments is the FEM simulation result at a single mesh size, namely, $m = 4$. Since mass density can be measured quite precisely and has negligible variability, we choose to work with the other three factors, namely, the length, L , thickness, t , and Young's modulus, E . Based on laboratory experience³² on the measurement variability of those three factors, we construct Table 4 for the first step of a DOE exercise:

Table 4 Factors and Two-Level Variability in DOE

Factor	Center Point Value	Percent Change ³²	(+1)	(-1)
$X1 = L$	0.232 mm	1.6 %	0.23571	0.22829
$X2 = t$	0.007 mm	2.5 %	0.00718	0.00682
$X3 = E$	169,158 MPa	0.1 %	169,327	168,989

In Table 5, we show the 8-run FEM simulation results and the full-factorial DOE with which we conducted simulations in both ABAQUS and ANSYS. Using a DATAPLOT subroutine for a 10-step analysis of DOE data presented in Part III, we first examine the output results for the 8-run ABAQUS data as shown in 5 of its 10 plots given by Figs. 7 through 11.

Table 5. ABAQUS 8-run Results for a Full-Factorial Two-Level Design

Order of Run	X1	X2	X3	ABAQUS (kHz)	ANSYS (kHz)
1	-1	-1	-1	182.119	182.306
2	+1	-1	-1	170.807	170.981
3	-1	+1	-1	191.692	191.888
4	+1	+1	-1	179.786	179.970
5	-1	-1	+1	182.301	182.488
6	+1	-1	+1	170.977	171.152
7	-1	+1	+1	191.883	192.080
8	+1	+1	+1	179.966	180.150

**Example 1 -
Continued**

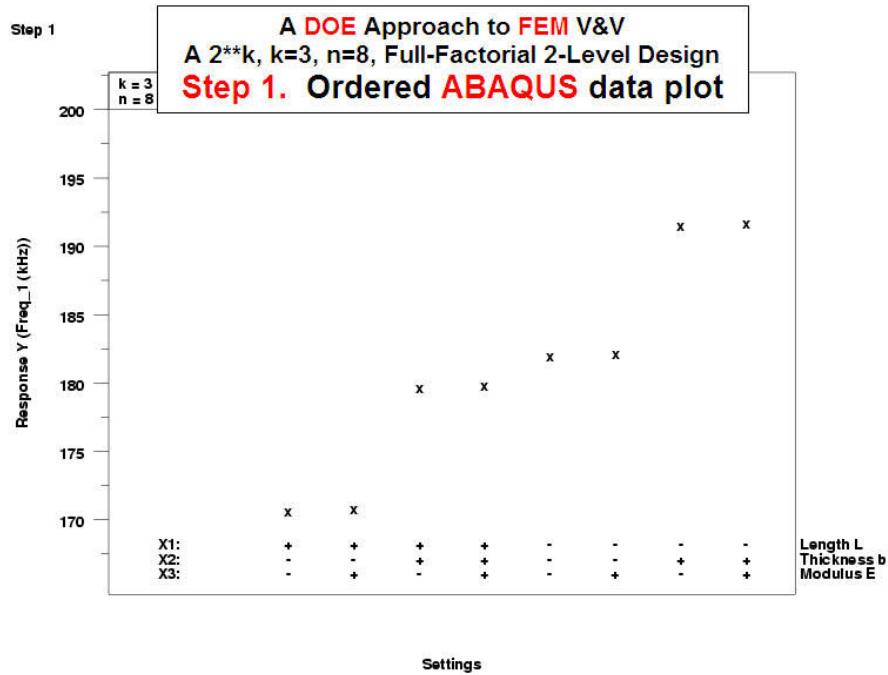


Fig. 7 First of ten plots by DATAPLOT showing the ABAQUS data as an ordered set. Note the table at the bottom of the plot being the transposed DOE matrix with re-ordered columns.

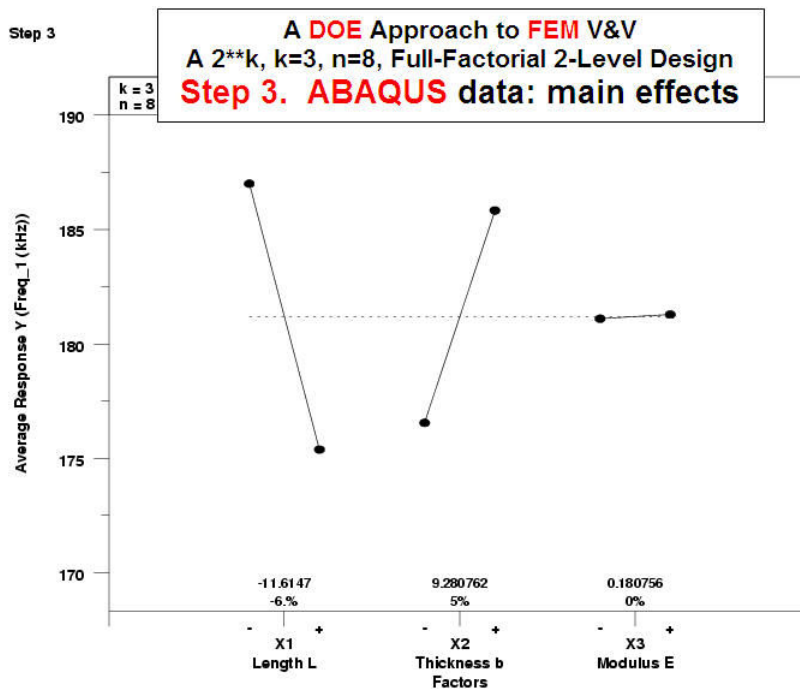


Fig. 8. Step 3 of a 10-step analysis of the ABAQUS data from 8 runs of experiments showing the main effects of the full factorial 2-level design (k = 3, n = 8). Note X1 and X2 are dominant.

Example 1 -
Continued

Step 4

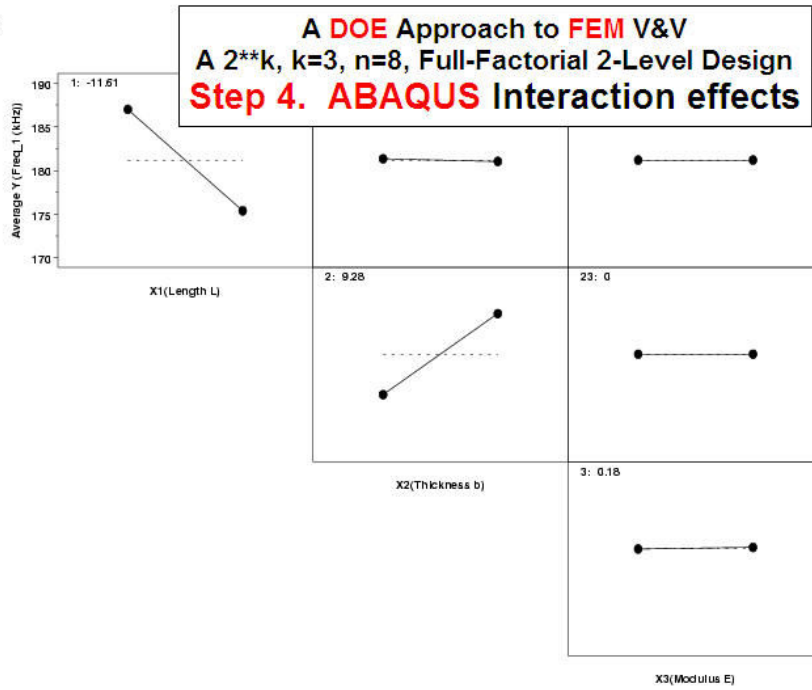


Fig. 9. Step 4 of a 10-step analysis of the ABAQUS data from 8 experimental runs showing the interaction effects of the full factorial design ($k=3, n=8$). Note the lack of interaction effects.

Step 7

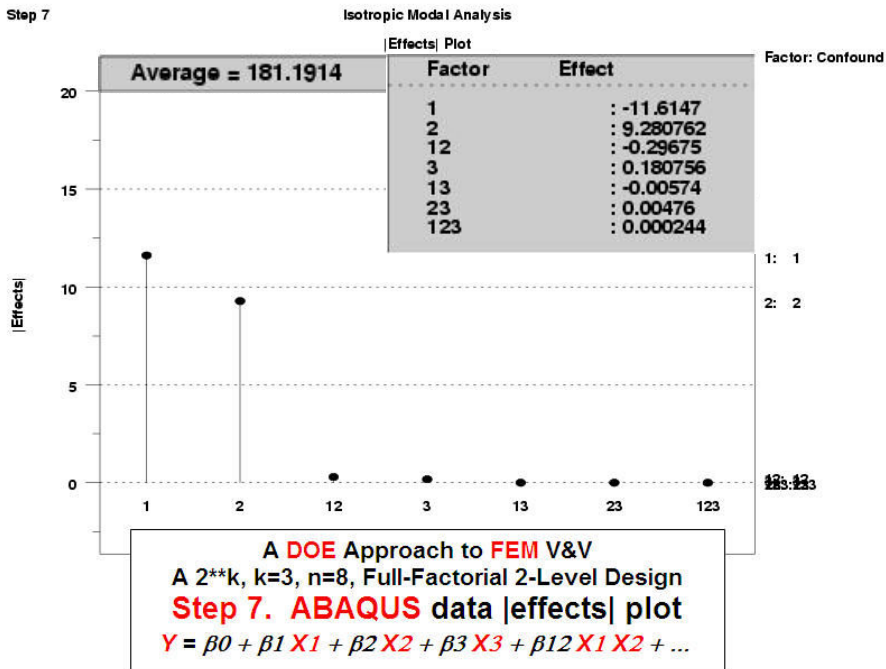


Fig. 10. Step 7 of a 10-step analysis of the ABAQUS data from 8 runs showing an ordered plot of the absolute values of the main ($\beta_1, \beta_2, \beta_3$) and interaction effects ($\beta_{12}, \beta_{13}, \beta_{23}, \beta_{123}$).

**Example 1 -
Continued**

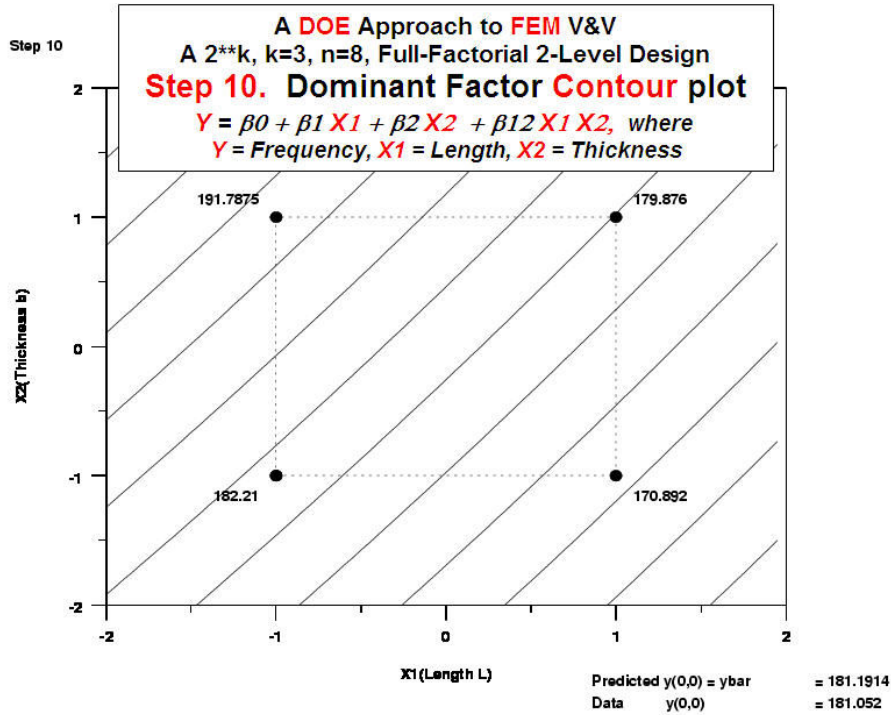


Fig. 11. Step 10 of an analysis of the ABAQUS data from 8 runs showing the contour plot of the 2 dominant factors, X1 and X2. The plane behavior of the plot shows β_{12} is negligible.

LEAST SQUARES MULTILINEAR FIT		Design_of_Experiment_FEM (ABAQUS)	
SAMPLE SIZE N = 9		3-Factor Full Factorial 2-Level Experiment	
NUMBER OF VARIABLES = 2		Vib. of Isotropic Elas. Cantilever Beam	
REPLICATION CASE			
REPLICATION STANDARD DEVIATION =		0.1279169	
REPLICATION DEGREES OF FREEDOM =		4	
NUMBER OF DISTINCT SUBSETS =		5	
PARAMETER ESTIMATES		(APPROX. ST. DEV.)	T VALUE
1	A0	181.176	(0.6923E-01) 2617.
2	A1 X1	-5.80737	(0.7343E-01) -79.08
3	A2 X2	4.64037	(0.7343E-01) 63.19
RESIDUAL STANDARD DEVIATION =		0.2077026	
RESIDUAL DEGREES OF FREEDOM =		6	
REPLICATION STANDARD DEVIATION =		0.1279169470	
REPLICATION DEGREES OF FREEDOM =		4	
LACK OF FIT F RATIO = 5.9095 = THE 93.6062% POINT OF THE			
F DISTRIBUTION WITH 2 AND 4 DEGREES OF FREEDOM			

Fig. 12. Sensitivity analysis of the 3-factor 8-run-plus-center-point ABAQUS data using a two-parameter (length and thickness) least square multilinear fit algorithm of DATAPLOT.

**Example 1 -
Continued**

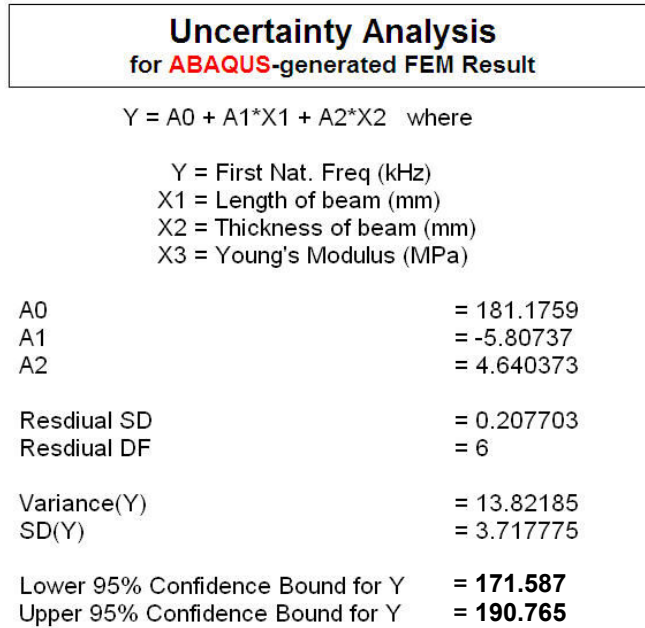


Fig. 13. Results of an uncertainty analysis generated by a DATAPLOT 10-step code showing that the first natural frequency of the bending of an isotropic elastic beam has a prediction 95% confidence interval of (171.587 kHz, 190.765 kHz) for the ABAQUS⁵ mesh-4 simulation.

In Fig. 7, we plot the 8-run ABAQUS data in an ordered set with the DOE matrix displayed at the bottom of the plot in a transposed matrix form. In Figs. 8 and 9, we exhibit the main and interaction effects of the analysis in a graphical form such that a quick inspection of the two figures gives us a feel as to how strong or weak are the relative magnitudes of the effects given by $\beta_1, \beta_2, \beta_3, \beta_{12}, \beta_{13},$ and β_{23} of eq. (2), Part II, Topic A. As a matter of fact, all of the coefficients, except β_0 , of eq. (2) for a full-factorial 8-run design are given in Fig. 10 in a box on the upper right corner of the plot. Furthermore, Fig. 10 is also a plot of the absolute values of those seven coefficients to show decisively that X_1 and X_2 are the two dominant factors, and X_3 and all two-term and three-term interactions are negligible. This interesting result allows us to simplify the model given in eq. (2) to a multilinear model of two factors, namely, $Y = A_0 + A_1 X_1 + A_2 X_2$. A graphical plot of this model is given in Fig. 11, a display of the estimated coefficients, $A_0, A_1,$ and A_2 , by a least square fit, in Fig. 12, and a summary of the ABAQUS 8-run DOE uncertainty analysis results is given in Fig. 13. The formula we used to calculate the prediction confidence intervals with the usual standard notation of the statistics literature, is given below (see, e.g., Nelson, Coffin and Copeland⁴³ [p. 179, eq. 5.3.2]):

$$\bar{y} \pm t(\alpha/2; n - 1) * s * (1 + 1/n)^{1/2} \tag{4}$$

We are now able to compare the estimated uncertainty of an ABAQUS simulation due to Class A and Class B errors. From Fig. 13, the estimated 95% upper and lower bounds of the frequency response, Y , are given by 190.765 and 171.587, respectively, or by 181.176 (9.589), where 9.589 is the 95% confidence half-interval. This value is two orders of magnitude larger than its counterpart, 0.096, given in Fig. 5 by a grid convergence least square fit algorithm.

Example 1 - Continued

To illustrate the difference between a full-factorial and a half-factorial design, we continue our investigation by running an ABAQUS 4-run experiment as shown in Table 6.

Table 6. ABAQUS 4-run Results for a Half-Factorial Two-Level Design

Order of Run	X1	X2	X3 (X1*X2)	ABAQUS (kHz)	ANSYS (kHz)
1	-1	-1	+1	182.301	182.488
2	+1	-1	-1	170.807	170.981
3	-1	+1	-1	191.692	191.888
4	+1	+1	+1	179.966	180.150

The half-factorial design is also given in Table 6, where the column under X3 is given by the product of the columns under X1 and X2.

In Fig. 14, we plot the main and two-term interaction effects of the experiment and observe that there are some two-term interactions that were not observed in a full-factorial experiment. This phenomenon is quantified in Fig. 15 where we discover that the coefficients, β_1 , β_2 , and β_3 , are now "confounded." For example, the correct value of β_2 given in Fig. 10 as -9.280762 , is now computed as -9.27501 , because the latter includes an effect known as β_{13} .

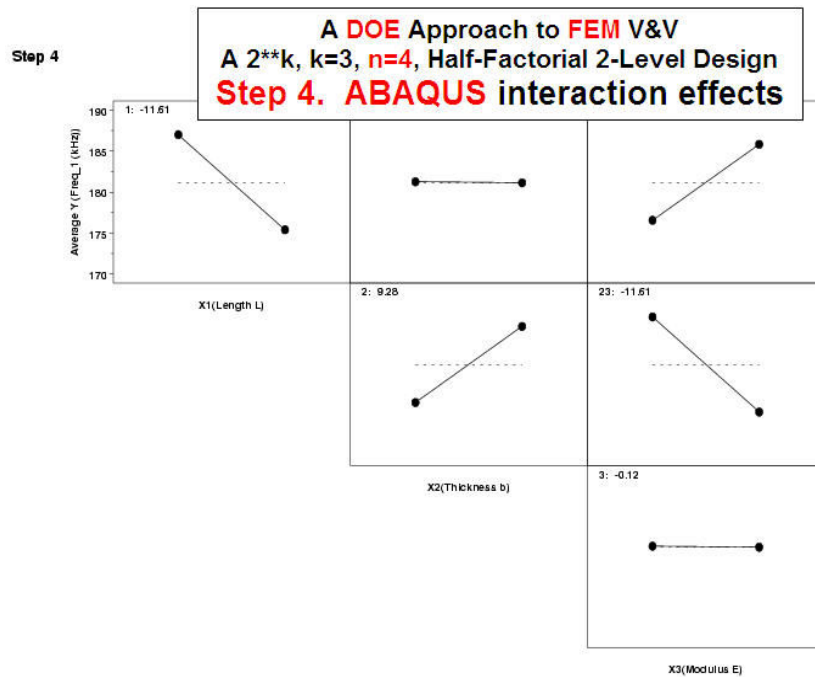


Fig. 14. Step 4 of a 10-step analysis of the ABAQUS data from 4 runs showing the interaction effects of the half-factorial design ($k = 3, n = 4$). Note the presence of two interaction effects.

**Example 1 -
Continued**

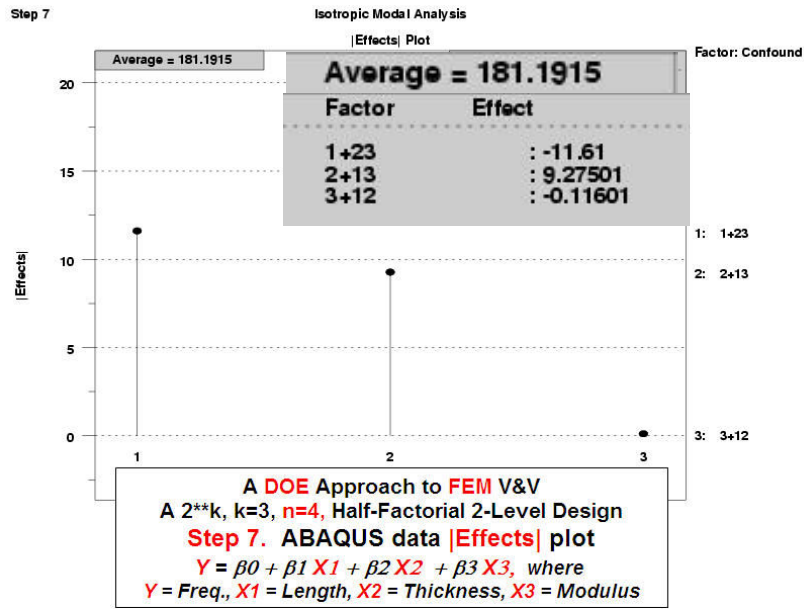


Fig. 15. Step 7 of a 10-step analysis of the ABAQUS data from 4 runs showing an ordered plot of the absolute values of a mixture of main ($\beta_1, \beta_2, \beta_3$) and interaction effects ($\beta_{12}, \beta_{13}, \beta_{23}$).

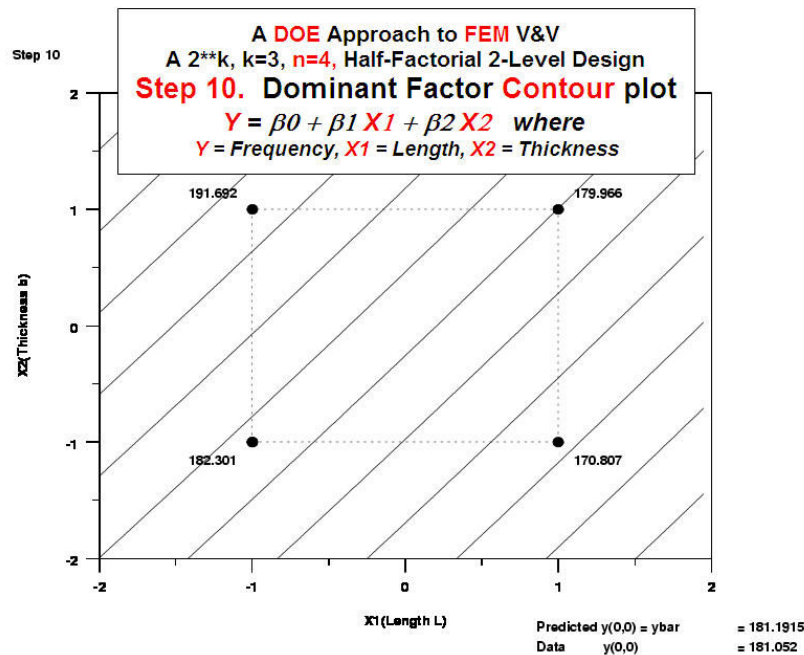


Fig. 16. Step 10 of an analysis of the ABAQUS data from 4 runs showing the contour plot of the 2 dominant factors, X1 and X2. The total no. of runs is not enough to support a model with interaction effects, so we ended up with no choice but a plane behavior of the contour plot.

**Example 1 -
Continued**

Uncertainty Analysis (ABAQUS, Fract Factorial)

A0	= 181.1636
A1	= -5.805
A2	= 4.6375
Residual SD	= 0.120468
Residual DF	= 2
Variance(Y)	= 13.80836
SD(Y)	= 3.71596
Lower 95% Confidence Bound for Y	= 163.649
Upper 95% Confidence Bound for Y	= 198.679

Fig. 17. Results of an uncertainty analysis generated by a DATAPLOT 10-step code showing that the first natural frequency of the bending of an isotropic elastic beam has a much wider 95% confidence interval, (163.649 kHz, 198.679 kHz), based on a half-factorial design with only 4 runs of the ABAQUS⁵ mesh-4 simulation, instead of the 8-run full factorial design.

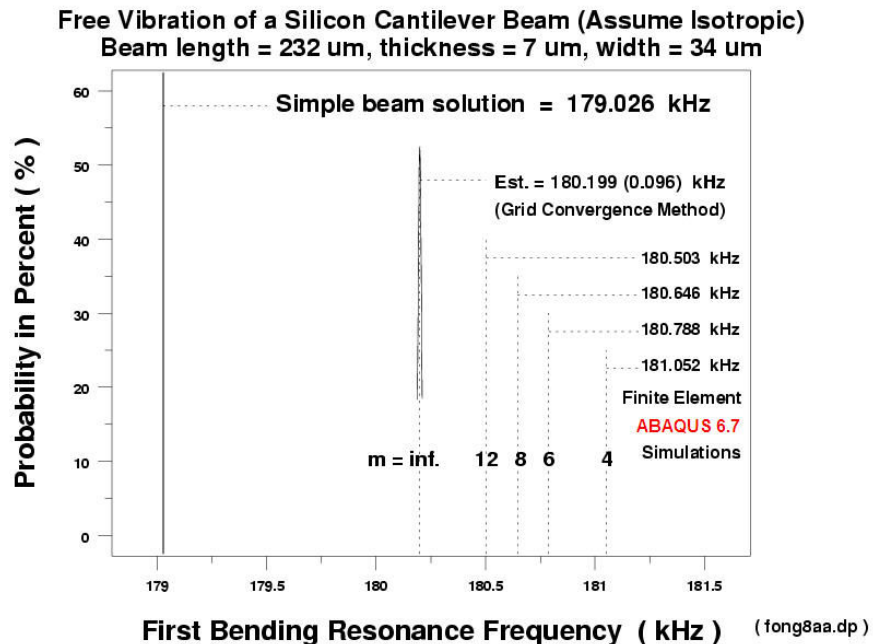


Fig. 18. A re-plot of Fig. 5 showing that the frequency with confidence half-interval, 180.199 (0.096) kHz, estimated from a least square approximation of an inverse-quadratic model of the 4-mesh ABAQUS grid convergence data, fails to match the theoretical solution of 179.026 kHz

Example 1 - Continued

Free Vibration of a Silicon Cantilever Beam (Assume Isotropic)
 Approach 1a: FEM (ABAQUS 6.7) with Design of Experiments

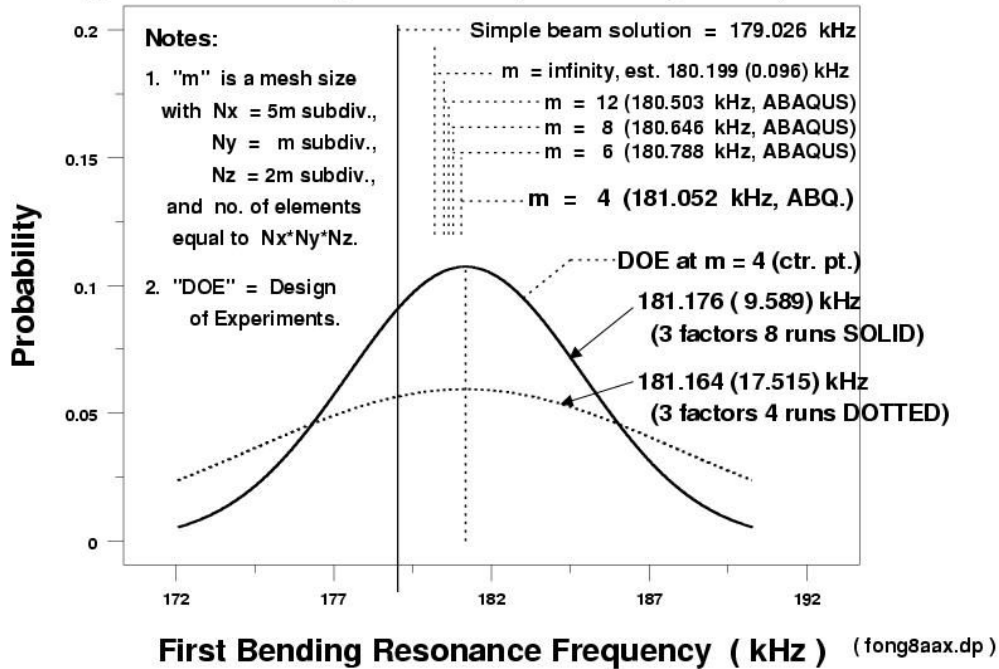


Fig. 19. Combining uncertainty analysis results of Fig. 5 (4-point grid convergence modeling), Fig. 13 (3-factor, 8-run, full factorial DOE on mesh-4 with center point) and Fig. 17 (3-factor, 4-run, half factorial DOE on mesh-4 with center point), we present a graphical representation of the three FEM simulation results in a probability vs. frequency plot, where the three results are, 180.199 (0.096) kHz, 181.176 (9.589) kHz, and 181.164 (17.515), respectively.

In Figs. 16 and 17, we find that contour plot and the uncertainty analysis of the simplified two-parameter model of a 4-run half-factorial design give quite different results from the same of the 8-run full-factorial one. For the half-factorial design, the lower and upper bounds of the 95% confidence estimates of the frequency are given by 163.649 and 198.679, or, in the standard expression of uncertainty, by 181.164 (17.515). A summary of the three uncertainty results for all ABAQUS runs is given in Figs. 18 and 19. Note the increase in the estimate of uncertainty from 9.589 to 17.515 when the DOE is changed from an 8-run full-factorial to a 4-run half-factorial one. The moral of the exercise is that *one needs more runs to reduce uncertainty*. This ends our example for finding the Class A errors.

Table 7 Estimated Mean and Variance of FEM Simulations using ABAQUS and ANSYS

	ABAQUS	ANSYS
Mean	$\bar{Y}_A = 181.176$	$\bar{Y}_B = 181.362$
Variance	$s_A^2 = 13.822$	$s_B^2 = 13.851$

*Example 1 -
Continued*

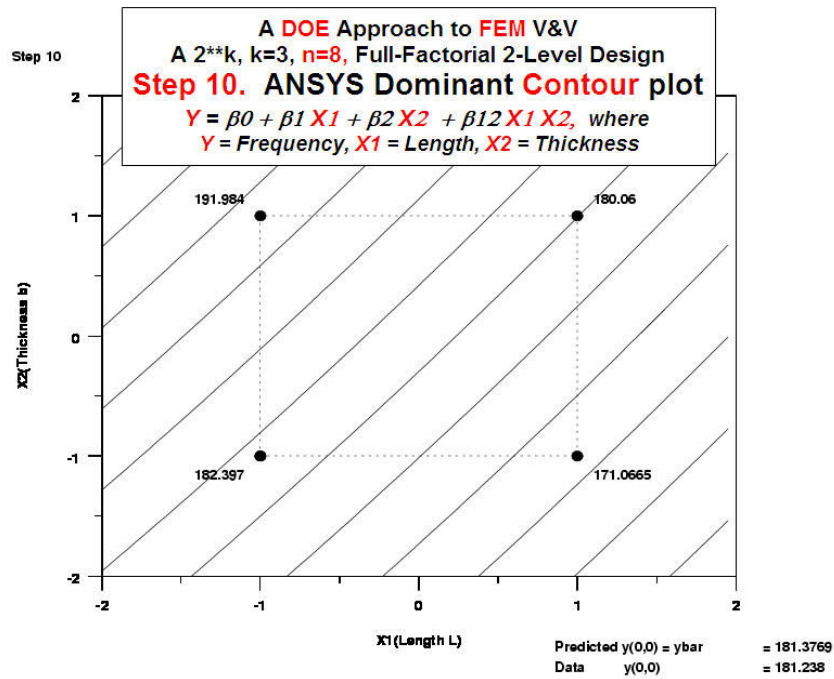


Fig. 20. Step 10 of an analysis of the ANSYS data from 8 runs showing the contour plot of the 2 dominant factors, X1 and X2. The plane behavior of the plot shows β_{12} is negligible.

Uncertainty Analysis
 for **ANSYS**-generated FEM Result

A0	= 181.3615
A1	= -5.81363
A2	= 4.645124
Residual SD	= 0.207796
Residual DF	= 6
Variance(Y)	= 13.85106
SD(Y)	= 3.7217
Lower 95% Confidence Bound for Y	= 171.762
Upper 95% Confidence Bound for Y	= 190.962

Fig. 21. Results of an uncertainty analysis generated by a DATAPLOT 10-step code showing that the first natural frequency of the bending of an isotropic elastic beam has a predicted 95% confidence interval of (171.762 kHz, 190.962 kHz) for the ANSYS⁶ mesh-4 simulation.

Example 1 - Continued

To address Class C error due to software implementation, we perform an identical FEM simulation experiment of an 8-run full factorial design using ANSYS (see Figs. 20 and 21). A summary of the DOE analysis results for both ABAQUS and ANSYS is given in Table 7.

Considering each FEM solution as a “Treatment” in a statistical experiment³⁷, we apply an analysis of variance (ANOVA) technique to obtain an equally-weighted consensus value of the two estimated variances and means as shown below:

Step 1. Calculate the consensus mean \bar{y} :

$$\bar{y} = (\bar{y}_A + \bar{y}_B) / 2 = 181.269 \text{ kHz.} \quad (5)$$

Step 2. Calculate the consensus variance, s^2 , using the formula given by Liu and Zhang⁴⁴ when the number of treatment is 2 and each weight equals 1/2 :

$$s^2 = \underbrace{(s_A^2 + s_B^2) / 2}_{[within-treatment]} + \underbrace{(\bar{y}_A - \bar{y})^2 / 2 + (\bar{y}_B - \bar{y})^2 / 2}_{[between-treatment]} \quad (6)$$

$$= 13.8365 + 0.0043 + 0.0043 = 13.8451 ,$$

and the consensus standard deviation $s = 3.7209 \text{ kHz}$.

Step 3. Calculate 95% confidence half-interval using the combined residual degrees of freedom equal to the sum of the residual degrees of freedom of Method A (ABAQUS) given in Fig. 12 and Method B (ANSYS) in Fig. 21, i.e.,

$$\begin{aligned} \text{Combined } Rdf &= (Rdf)_A + (Rdf)_B \\ &= 6 + 6 = 12. \end{aligned} \quad (7)$$

From the t -distribution table (see, e.g., Nelson, Coffin, and Copeland⁴³, p.444, Table B-2), we obtain $t(0.025, 12) = 2.179$. For $n = 9 + 9 = 18$, the 95% confidence half-interval is given by:

$$95\% \text{ prediction half-interval} = 2.179 * s * (1 + 1/18)^{1/2} = 8.330 \text{ kHz.}$$

In summary, the 3 error estimates in the form of prediction 95% confidence half-intervals are:

For ABAQUS Class B error by 4-mesh grid convergence method: $Y = 180.199 (0.096)$.

For DOE-ABAQUS Class A error on a single mesh (Mesh-4): $Y = 181.176 (9.589)$.

For DOE-ABAQUS & DOE-ANSYS Classes A & C errors on Mesh-4: $Y = 181.269 (8.330)$.

In the next example, for which there is no known theoretical solution, we will demonstrate how to combine Classes B (mathematical) and C (software implementation) as well as A and C errors.

Example 2 Vibration of a Single-Crystal Silicon Cantilever Beam

In experiments and simulations on the resonance frequencies of the single-crystal silicon cantilever beam in an atomic force microscope (see, e.g., Rabe, et al⁴⁵, Kester, et al⁴⁶, etc.), as shown in Fig. 22, a major discrepancy was reported by Hurley, et al⁴⁷ [p.2347, Table 1] on the two lowest natural bending resonance frequencies of such beam in two different shapes, rectangular and dagger.

For instance, the first natural frequency for a rectangular shape⁴⁷ with nominal lengths, 0.223/0.232 mm, and thickness, 0.0081 mm, was found to be 180.8 (0.2) kHz (experimental) and 189.7 kHz (extrapolated to 0.0081 mm thickness from an ANSYS FEM solution of 180.8 kHz for 0.00772 mm thickness by assuming eq. (1) holds for the extrapolation). The 4.9% difference between the experimental (180.8) and the ANSYS FEM solution (189.7) needs to be augmented by a comparison of the uncertainty in the measured and the predicted values. Unfortunately, the ANSYS simulation reported by Hurley, et al⁴⁷ did not include an uncertainty estimate. A subsequent investigation by Fong, et al³² reported results with several different uncertainty estimates, of which a few were based on DOE. One such DOE-based estimate is presented here as an example of a new approach to FEM uncertainty estimation.

As mentioned earlier in this paper, the exact solution of all resonance frequencies of a cantilever beam in linear isotropic elasticity is well known (see, e.g., Timoshenko and Young⁴⁰ [p. 338], and Clough and Penzien⁴¹ [p. 380] as shown in Fig. 1). However, the same for a single-crystal silicon beam modeled as an orthotropic material because of its orientation does not exist in the literature (see, e.g., Fong, et al³²), even though a series solution for the static case of an orthotropic cantilever of rectangular cross-section subject to an end load is known (see, e.g., Lekhnitskii⁴⁸).

The existence of an exact solution for an isotropic free-vibration problem and the lack of the same for an orthotropic one provided an opportunity for Fong, et al³² to (a) search for an approximate solution with uncertainty bounds for the orthotropic problem and (b) apply a metrology-based approach to the verification of the solution by examining uncertainty of all three classes listed in Part I. A typical plot of the free vibration analysis of an anisotropic elastic cantilever beam using a specific mesh design (e.g., Mesh size $m = 4$) is given in Fig. 23.

Let us begin with Class B (mathematical) error estimation. Similar to the 8-node grid convergence experiment we presented in Example 1, we choose to work with four mesh designs, namely, Mesh-4, Mesh-6, Mesh-8, and Mesh-10. A typical plot of the h^2 -convergence of one FEM software package, LS-DYNA, is given in Fig. 24. A least square fit of those data for an inverse-quadratic model using DATAPLOT¹ allows us to extrapolate the model to Mesh-infinity and obtain a predicted value of the first frequency with 95% confidence half-interval equal to 179.349 ± 0.131 kHz.

Unlike the case of the free vibration of an isotropic elastic cantilever beam, the extrapolated frequency result shown in Fig. 24 cannot be compared with a theoretical solution, and thus we do not have the means to determine the absolute error of Class B (mathematical). Using a metrological approach, we could estimate the combined errors of Class B (mathematical)

Example 2 - Continued

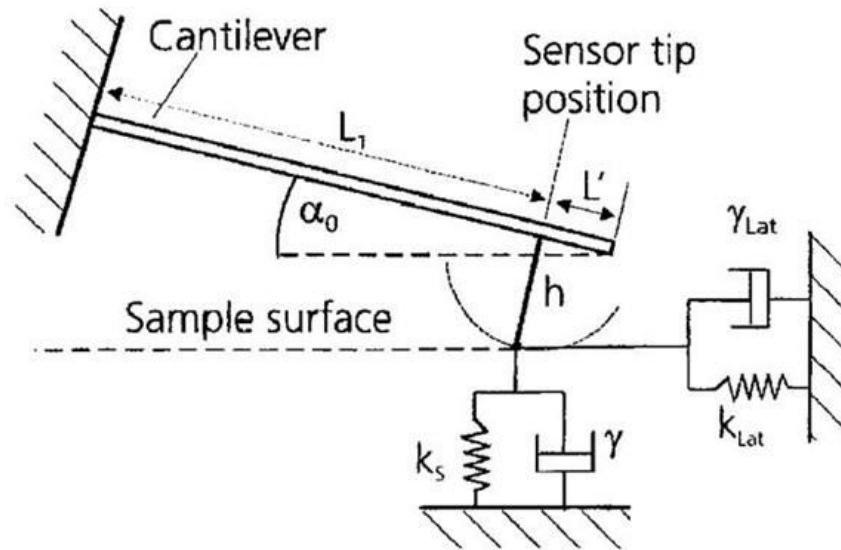


Fig. 22. Typical geometry of a single-crystal silicon cantilever beam with the location of a tip in contact with the surface of a sample in an atomic force microscope (after Kester, Rabe, Presmanes, Tailhades, and Arnold⁴⁶ [p. 1277, Fig. 3]).

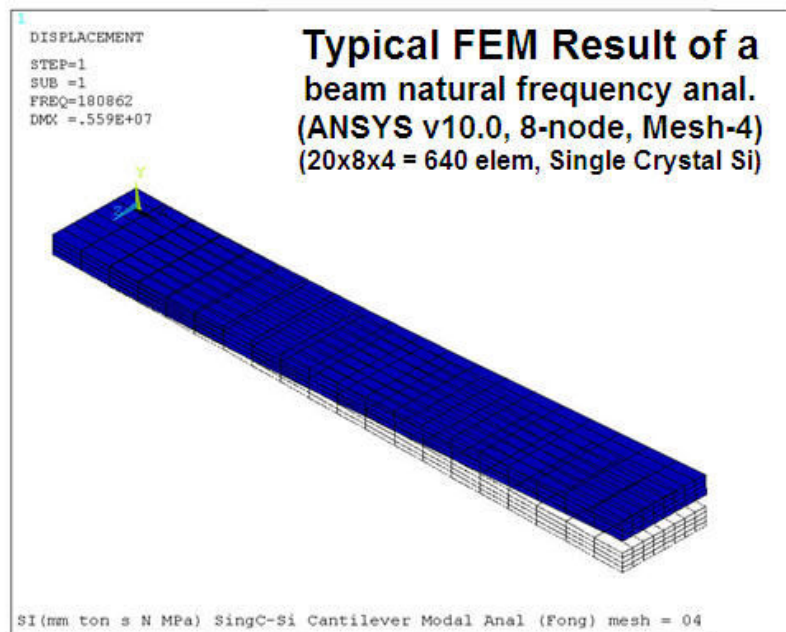


Fig. 23. Typical FEM result of a beam natural frequency analysis using a FEM package named ANSYS⁵, version 10.0, with an 8-node element type and a mesh design (total 640 elements).

Example 2 - Continued

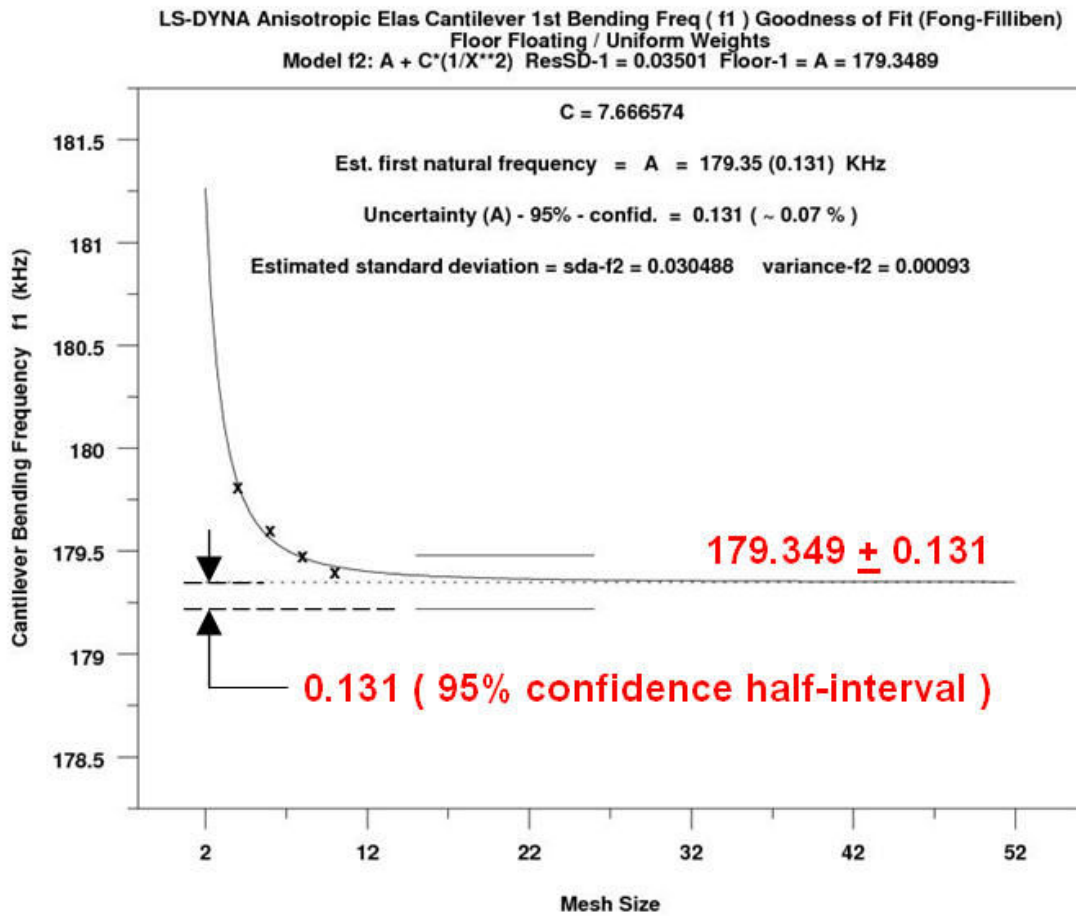


Fig. 24. A typical plot of the h^2 -convergence of the simulation results of one FEM software package, LS-DYNA⁶, for an 8-node 4-mesh-design ($m = 4, 6, 8, 10$) grid convergence experiment. A least square fit of those data for an inverse-quadratic model using DATAPLOT¹ allows us to extrapolate the model to Mesh-infinity and obtain a predicted value of the first frequency with 95% confidence half-interval equal to 179.349 ± 0.131 kHz.

and Class C (software implementation) by performing same exercises using different FEM packages and element types. In Fig. 25, we show³² a summary plot of four such exercises, namely, ABAQUS (8-node element type C3D8I), ABAQUS (20-node element type C3D20), ANSYS (8-node element type ST64 for anisotropic solid), and LS-DYNA (8-node type 002). A summary of the extrapolated means and predictionh 95% confidence half-intervals of those four exercises are given below:

	Estimated Mean	Prediction 95% Half-Interval
ABAQUS (8-node C3D8I):	179.218 kHz	0.087 kHz
ABAQUS (20-node C3D20):	179.128	0.028
ANSYS (8-node type ST64):	180.321	0.087
LS-DYNA (8-ndoe type 002):	179.349	0.131

Example 2 - Continued

From Fig. 18, we observe that for the case of an isotropic elastic beam, the grid-convergence method yields an extrapolated mean frequency (180.199 kHz) larger than the theoretical solution (179.026 kHz). Assuming this is also true for an anisotropic elastic beam where the unknown theoretical solution is also to the left of the FEM simulations, the four-plot diagram in Fig. 25 shows that among the four FEM results, the absolute error (Class B) of ANSYS (ST64) is the largest. This observation provides us a basis for assigning weights to each of the four simulations by assuming that one can calculate weights as proportional to the inverse of the product of (a) the absolute value of the distance from the theoretical solution to the extrapolated frequency, and (b) the standard deviation of the extrapolated frequency, if such a set of exercises is carried out for the isotropic elastic beam case. Using a method by Liu and Zhang⁴⁴, Fong, et al³² showed that the combined weighted result of the frequency estimation with prediction 95% confidence intervals is given by 179.385 (0.929) kHz.

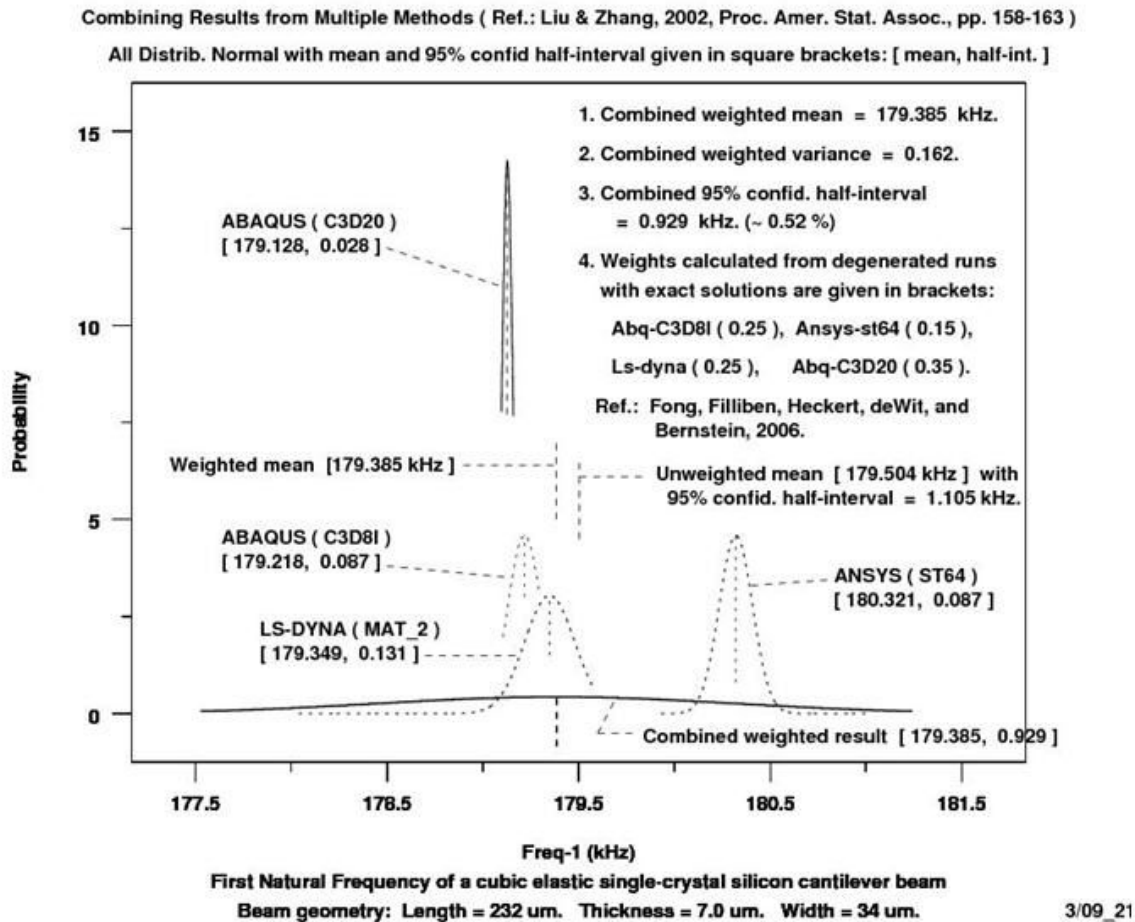


Fig. 25. Estimated Means and 95% Confidence Half-Intervals of First Natural Frequency of a Single-Crystal Silicon Cantilever by four FEM methods, namely, ABAQUS (Element C3D8I), ANSYS (Element 64), LS-DYNA (Element 002), and ABAQUS (Quadratic Element C3D20). Unweighted (i.e., equal weights) & “weighted” means & prediction confidence half-intervals are also displayed for comparison.

Example 2 - Continued

Table 8. A 5-variable 8-run fractional orthogonal design for two-level experiments based on Box, Hunter, and Hunter³⁷ [p. 420] and a more general design [same reference, p. 410].

run	variable				
	1	2	3	4	5
1	-	-	-	+	-
2	+	-	-	+	+
3	-	+	-	-	+
4	+	+	-	-	-
5	-	-	+	-	+
6	+	-	+	-	-
7	-	+	+	+	-
8	+	+	+	+	+

Table 9. List of 5 input parameters (length, thickness, and 3 elastic constants) for a 5-variable, 9-run fractional orthogonal design (with center point) of a FEM experiment in computing the first natural frequency of a single-crystal silicon cantilever beam. Three elastic constants for the center run 0 in silicon before rotation, given here in solid line brackets, are based on McSkimin and Andreatch⁴⁹.

Effect No.	1	2	3	4	5				
	L = length	h = thickness	c ₁₁	c ₁₂	c ₄₄				
Effect-1 (based on NIST-Richard-Gates)	(+, -)1.6%								
Effect-2 (based on NIST-Donna-Hurley)		(+, -) 2.5%							
Effect-3,4,5 (based on McSkimin-Andreatch)			(+, -) 0.1%	(+, -)0.25%	(+, -)0.05%				
Center	(- - - + -)	(+ - - + +)	(- + - - +)	(+ + - - -)	(- - + - +)	(+ - + - -)	(- + + + -)	(+ + + + +)	
Run_0	1	2	3	4	5	6	7	8	
Factor									
L	0.232	0.228288	0.235712	0.228288	0.235712	0.228288	0.235712	0.228288	0.235712
h	0.007	0.006825	0.006825	0.007175	0.007175	0.006825	0.006825	0.007175	0.007175
c ₁₁	165755	165589	165589	165589	165589	165921	165921	165921	165921
c ₁₂	63912.1	64071.9	64071.9	63752.3	63752.3	63752.3	63752.3	64071.9	64071.9
c ₄₄	79619.0	79579.2	79658.8	79658.8	79579.2	79658.8	79579.2	79579.2	79658.8

Example 2 - Continued

Table 10. Solution of first natural frequency (kHz) of a single-crystal silicon cantilever by a finite element method (FEM) based on (1) a 5-factor 8-run-plus-center-point fractional orthogonal design of experiments with prescribed input variability, (2) a commercially-available FEM package named ANSYS⁵, version 10.0, and (3) four specific mesh sizes, m-6 (30 equal divisions in length, 6, in thickness, and 12, in width, or 30 x 6 x 12), m-8 (40 x 8 x 16), m-10 (50 x 10 x 20), and m-12 (60 x 12 x 24).

	Effect No.								
(Variability in all input parameters is 2-sigma)	1	2	3	4	5				
	L = length	h = thickness	c ₁₁	c ₁₂	c ₄₄				
Effect-1 (based on NIST-Richard-Gates)	(+, -) 1.6%								
Effect-2 (based on NIST-Donna-Hurley)		(+,-) 2.5%							
Effect-3, 4, 5 (based on McSkimin-Andreatch)			(+,-) 0.1%	(+,-) 0.25%	(+,-) 0.05%				
ANSYS	Center	(- - - + -)	(+ - - + +)	(- + - - +)	(+ + - - -)	(- - + - +)	(+ - + - -)	(- + + + -)	(+ + + + +)
	Run 0	1	2	3	4	5	6	7	8
Mesh									
m-6	180.588	181.692	170.536	191.158	179.233	181.961	170.608	191.180	179.348
m-8	180.459	181.562	170.414	191.024	179.106	181.832	170.487	191.044	179.220
m-10	180.387	181.489	170.345	190.947	179.034	181.759	170.418	190.967	179.148
m-12	180.341	181.442	170.301	190.899	178.989	181.713	170.374	190.919	179.102

So far, we have discussed the combination of Class B (mathematical) and Class C (software implementation) errors to obtain a frequency estimate with uncertainty bounds for an anisotropic elastic cantilever beam. But we observe from Example 1 that the uncertainty for Class A errors (physical) of a FEM simulation, when evaluated via the method of DOE, is several orders of magnitude larger in the case of an isotropic elastic beam. We will now conduct a DOE for the anisotropic beam to see if the same is true.

In Table 8, we first adopt a 5-variable and 2⁵⁻² fraction (X₄=X₂*X₃, X₅=X₁*X₂*X₃) orthogonal design for two-level experiments (see Box, Hunter, and Hunter³⁷ [p.420]) in order to evaluate Class A errors for a specific FEM mesh design, namely, *m* = 12. In Table 9, we first list the variability of each of the five factors, namely, length, thickness, and the three elastic constants c₁₁, c₁₂, and c₄₄, of a single-crystal (cubic) silicon beam. We then show the values of those five factors needed for us to make 9 runs (8 for DOE plus one center point) of FEM simulations. In Table 10, we show the frequency responses of an ANSYS simulation experiments at mesh sizes 6, 8, 10, and 12.

For this example, we will only carry out a DOE exercise for mesh size 12, as outlined in red in Table 10. Using DATAPLOT to conduct a 10-step analysis of the DOE data of mesh 12, we show in Fig. 26 a plot of the main effects, with X₁ (length) and X₂ (thickness) singled out as obviously dominant. Unfortunately, we observe in Fig. 27 that there are confounding effects in the interaction matrix. In Fig. 28, we observe that the main effect of X₁ is confounded with X₂*X₄ and X₃*X₅. However, since X₃, X₄, and X₅ have negligible effects (see Fig. 26), the confounding effects of X₂*X₄ and X₃*X₅ within X₁ are also negligible. Such an argument allows us to simplify the 5-factor model to a 2-factor model as shown in Fig. 29. A least square multi-linear fit of the 9 data points is given in Fig. 30, and a summary of the uncertainty analysis results is given in Fig. 31. For ANSYS mesh-12 simulation, frequency = 180.453 (9.453) kHz.

**Example 2 -
Continued**

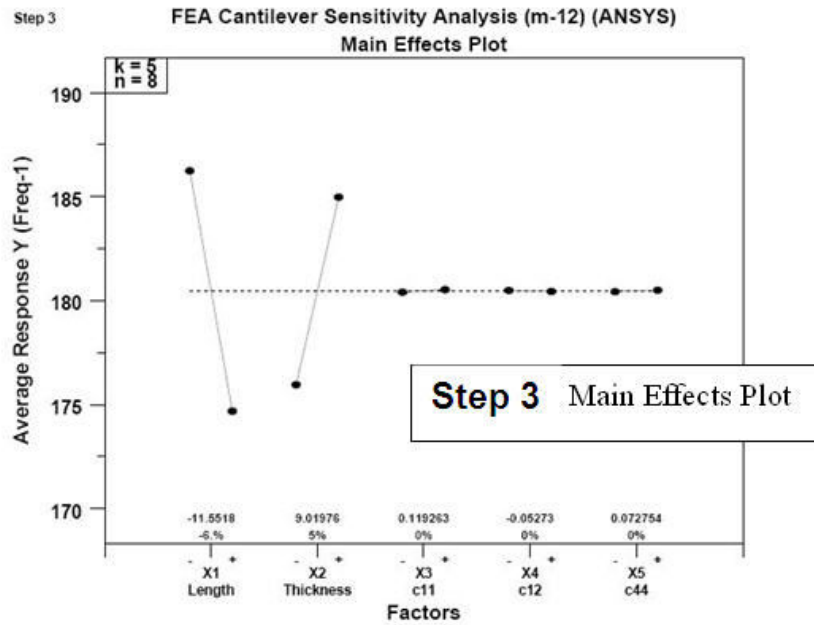


Fig. 26. Step 3 of a 10-step analysis (Ref. 39, Chap. 5, Sect. 5.5.9, pp. 313-412) of the data from 8 runs of experiments showing the main effects of the fractional factorial design.(k =5, n =8).

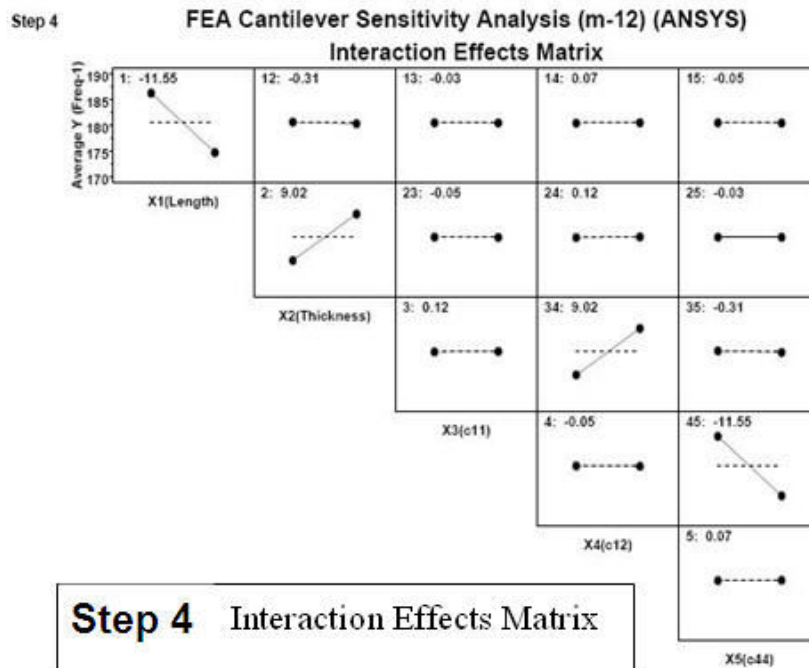


Fig. 27. Step 4 of a 10-step analysis (Ref. 39, Chap. 5, Sect. 5.5.9, pp. 313-412) of the data from 8 experimental runs showing the interaction effects of the fractional factorial design.(k =5, n =8).

Example 2 - Continued

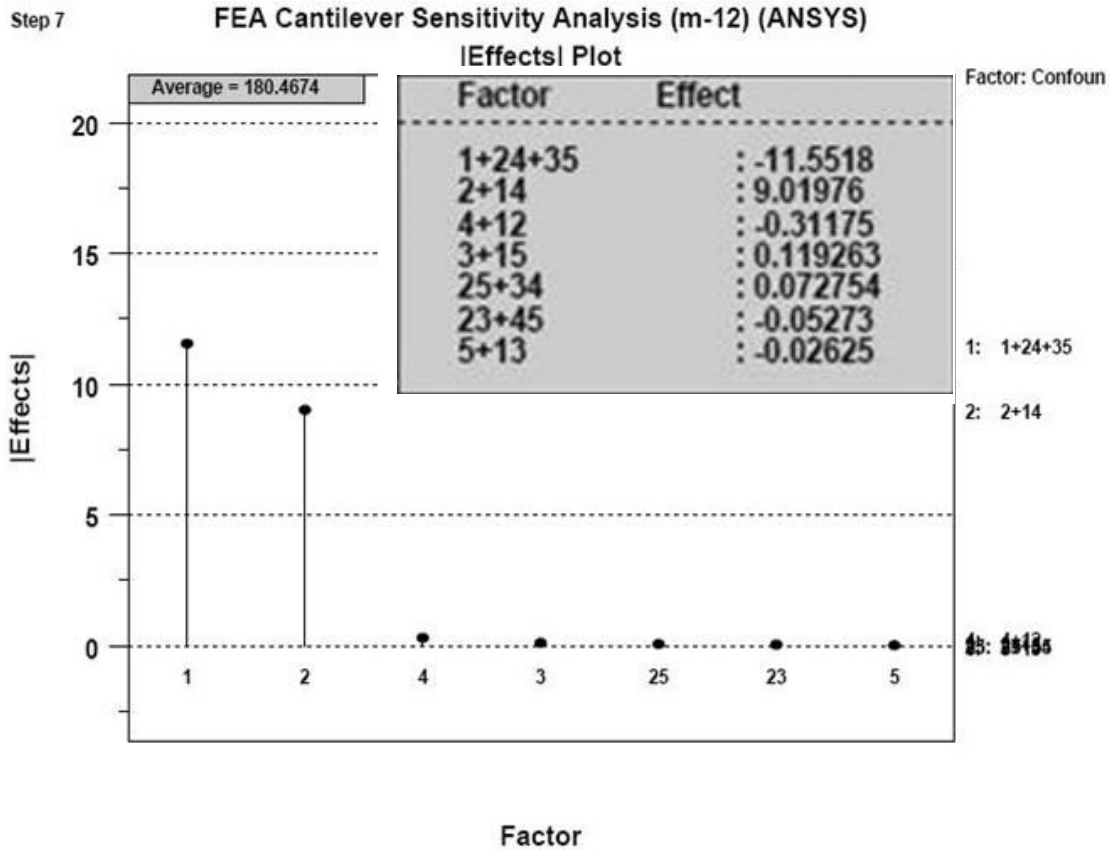


Fig. 28. Step 7 of a 10-step analysis of the ANSYS data from 8 runs showing an ordered plot of the absolute values of the main ($\beta_1, \beta_2, \beta_3, \beta_4, \beta_5$) and interaction effects.

Let us pause for what we have accomplished so far. We have obtained only the uncertainty estimate of the Class A error (physical) for one FEM software package, namely, ANSYS. We observe from Example 1 that a different package may not yield identical result, so we decided to make another set of experiment using LS-DYNA. In Table 11, the 9-run response values for LS-DYNA mesh-6 through mesh-12 are given. Again, we only choose to work with mesh-12, and a 10-step DOE-based analysis yields a similar output with Fig. 32 showing the least square multi-linear fit of the 9 response data by a function of two variables, and Fig. 33, the uncertainty analysis results. For LS-DYNA mesh-12 simulation, first frequency = 179.451 (9.393) kHz.

We are now ready to combine Classes A (physical) and C (software implementation) errors for two FEM software packages using the following individual estimates:

	ANSYS	LS-DYNA
Mean	$\bar{Y}_A = 180.453$	$\bar{Y}_B = 179.451$
Variance	$s_A^2 = 13.432$	$s_B^2 = 13.261$

Example 2 - Continued

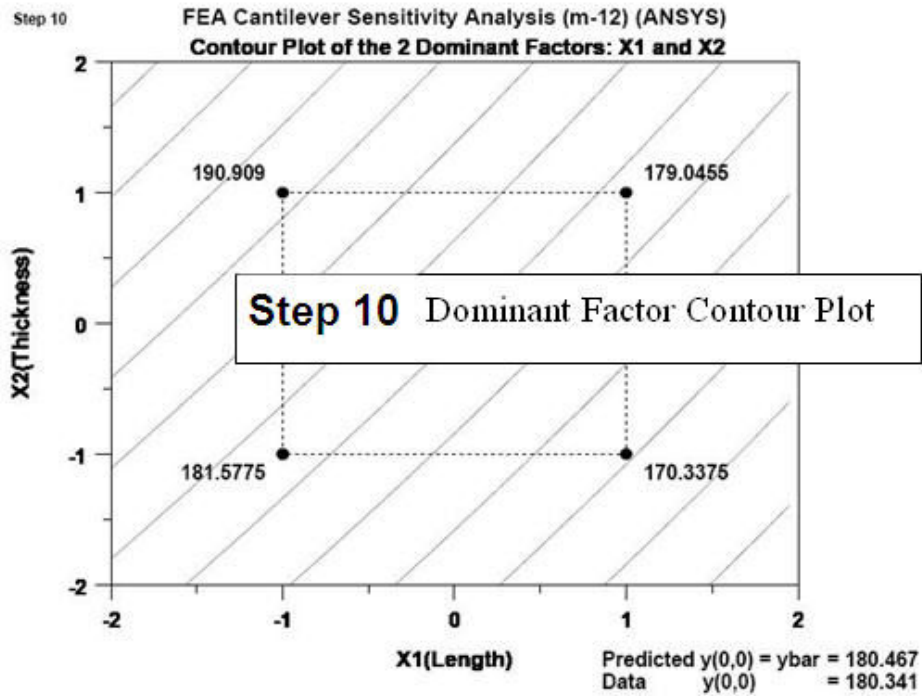


Fig. 29. Step 10 of a 10-step analysis (Ref. 39, Chap. 5, Sect. 5.5.9, pp. 313-412) of the data from 8 runs of experiments showing the contour plot of the 2 dominant factors, X1 and X2.

LEAST SQUARES MULTILINEAR FIT			
SAMPLE SIZE N	=	9	
NUMBER OF VARIABLES	=	2	
REPLICATION CASE			
REPLICATION STANDARD DEVIATION	=	0.1072021	
REPLICATION DEGREES OF FREEDOM	=	4	
NUMBER OF DISTINCT SUBSETS	=	5	
	PARAMETER ESTIMATES	(APPROX. ST. DEV.)	T VALUE
1	A0	180.453	(0.6866E-01) 2628.
2	A1 X1	-5.77588	(0.7282E-01) -79.32
3	A2 X2	4.50988	(0.7282E-01) 61.93
RESIDUAL STANDARD DEVIATION	=	0.2059687	
RESIDUAL DEGREES OF FREEDOM	=	6	
REPLICATION STANDARD DEVIATION	=	0.1072020605	
REPLICATION DEGREES OF FREEDOM	=	4	
LACK OF FIT F RATIO = 9.0743	=	THE 96.7384% POINT OF THE	
F DISTRIBUTION WITH 2 AND 4		DEGREES OF FREEDOM	

Fig. 30. Sensitivity analysis of the ANSYS⁵ mesh-12 design of experiment (DOE) data using a two-parameter (length and thickness) least square fit algorithm of a statistical software package named DATAPLOT¹.

Example 2 - Continued

A0	= 180.4533
A1	= -5.77588
A2	= 4.509878
Residual SD	= 0.205969
Residual DF	= 6
Variance(Y)	= 13.432
SD(Y)	= 3.66497
Lower 95% Confidence Bound for Y	= 171.000
Upper 95% Confidence Bound for Y	= 189.906

Fig. 31. A summary of the uncertainty results generated by a DATAPLOT 10-step DOE analysis code showing that the first natural frequency of the elastic bending of a single-crystal silicon beam has a prediction 95% confidence interval of (171.000 kHz, 189.906 kHz) for the ANSYS⁵ mesh-12 simulation.

Table 11. Solution of first natural frequency (kHz) of a single-crystal silicon cantilever by a finite element method (FEM) based on (1) a 5-factor 8-run-plus-center-point fractional orthogonal design of experiments with prescribed input variability, (2) a commercially-available FEM package named LS-DYNA⁶, version 970, and (3) four specific mesh sizes, m-6 (30 equal divisions in length, 6, in thickness, and 12, in width, or 30 x 6 x 12), m-8 (40 x 8 x 16), m-10 (50 x 10 x 20), and m-12 (60 x 12 x 24).

		Effect No.									
		1		2		3		4		5	
		L = length		h = thickness		c ₁₁		c ₁₂		c ₄₄	
Effect-1 (based on NIST-Richard-Gates)		(+, -)1.6%									
Effect-2 (based on NIST-Donna-Hurley)				(+, -) 2.5%							
Effect-3, 4, 5 (based on McSkimin-Andreatch)						(+, -) 0.1%		(+, -)0.25%		(+, -)0.05%	
Center		(- - - + -)	(+ - - + +)	(- + - - +)	(+ + - - -)	(- - + - +)	(+ - + - -)	(- + + + -)	(+ + + + +)		
Run 0		1	2	3	4	5	6	7	8		
Mesh											
m-6	179.596	180.663	169.602	190.103	178.275	180.940	169.681	190.122	178.386		
m-8	179.471	180.536	169.481	189.972	178.151	180.814	169.563	189.990	178.261		
m-10	179.392	180.456	169.406	189.889	178.074	180.736	169.489	189.907	178.183		
m-12	179.339	180.402	169.355	189.834	178.022	180.683	169.439	189.852	178.131		

LS-DYNA

Example 2 - Continued

```
LEAST SQUARES MULTILINEAR FIT
SAMPLE SIZE N           =    9
NUMBER OF VARIABLES     =    2
REPLICATION CASE
REPLICATION STANDARD DEVIATION = 0.1108061
REPLICATION DEGREES OF FREEDOM = 4
NUMBER OF DISTINCT SUBSETS = 5

      PARAMETER ESTIMATES      (APPROX. ST. DEV.)      T VALUE
1 A0          179.451      (0.6885E-01)      2606.
2 A1   X1      -5.72800    (0.7303E-01)      -78.44
3 A2   X2       4.49500    (0.7303E-01)       61.55

RESIDUAL STANDARD DEVIATION = 0.2065545
RESIDUAL DEGREES OF FREEDOM = 6
REPLICATION STANDARD DEVIATION = 0.1108061448
REPLICATION DEGREES OF FREEDOM = 4
LACK OF FIT F RATIO = 8.4247 = THE 96.3193% POINT OF THE
F DISTRIBUTION WITH 2 AND 4 DEGREES OF FREEDOM
```

Fig. 32. Sensitivity analysis of the LS-DYNA⁶ mesh-12 design of experiment (DOE) data using a two-parameter (length and thickness) least square fit algorithm of a statistical software package named DATAPLOT¹.

Uncertainty Analysis

```
A0          = 179.4508
A1          = -5.728
A2          = 4.495003
Residual SD = 0.206555
Residual DF = 6
Variance(Y) = 13.26087
SD(Y)       = 3.641548
Lower 95% Confidence Bound for Y = 170.058
Upper 95% Confidence Bound for Y = 188.844
```

Fig. 33. A summary of the uncertainty results generated by a DATAPLOT 10-step DOE analysis code showing that the first natural frequency of the elastic bending of a single-crystal silicon beam has a prediction 95% confidence interval of (170.058 kHz, 188.844 kHz) for the LS-DYNA⁶ mesh-12 simulation.

Example 2 - Continued

Again, as in Example 1, we consider each FEM solution as a "Treatment" in statistical experiment, and apply an analysis of variance (ANOVA) technique in three steps to obtain an equally-weighted consensus value of the two estimated variances and means. The method of combining Classes A (physical) and C (software packages) errors yields an estimate of the mesh-12 frequency with a prediction 95% confidence half-interval as 179.952 (8.254) kHz. A plot of comparing the multiple FEM DOE estimate (for $t = 0.007$ mm) with the experimental plus ANSYS simulation (for $t = 0.0081$ mm)⁴⁷ is given in Fig. 34.

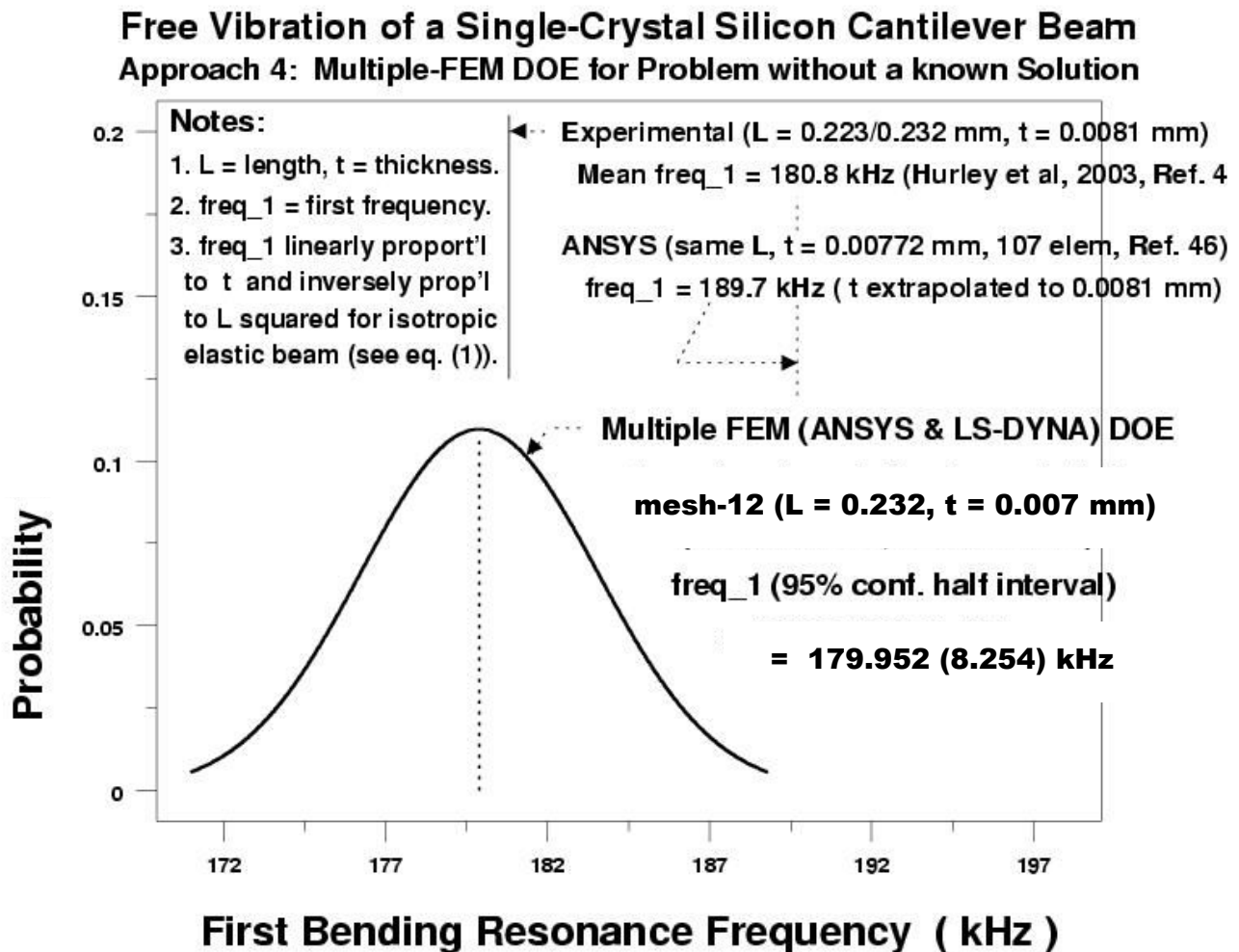


Fig. 34. A plot of comparing the multiple FEM DOE estimate (for $L = 0.232$ mm, $t = 0.007$ mm) with the experimental plus ANSYS simulation (for $L = 0.223/0.232$ mm, $t = 0.0081$ mm)⁴⁷. Note that without a known theoretical solution, the comparison is only qualitative, because a correct comparison requires all simulations to have the same L and t as those associated with the experiment.

Significance and Limitations of the DOE Approach

The DOE approach to an uncertainty estimation of FEM simulations, as presented in this paper with two examples, is significant for at least two reasons:

- (1) It provides an alternative approach to uncertainty estimation of mathematical modeling and simulation where the traditional approach of using Monte Carlo method becomes cost-prohibitive as the degrees of freedom per simulation go as high as hundreds of thousands or more in most FEM simulations.
- (2) It provides a new approach for a FEM user to translate his or her understanding of the variability of a problem to a quantitative expression of uncertainty in FEM results such that a better insight on many of the unknown features, e.g., constitutive equation, boundary condition, etc., may be gained before making decisions on new physical experiments.

In addition, the DOE approach provides a user with a method to rank the importance of various factors and to simplify a complex model to a manageable size.

There are, clearly, many limitations to this approach. The first and foremost is the loss of accuracy when many factors are confounded with interactions in a fractional factorial design. There is also a need to elevate the two-level experiment to three- or higher-level ones, but that will increase the computing cost significantly to render the approach not as useful.

Conclusion

As a deterministic computational method of simulation, finite element method (FEM) has been a valuable tool in both engineering and science ever since computer was introduced in the 1950s. Recent rapid advances in computer hardware and memory have made it possible to address the practical but hard question of delivering FEM simulations with uncertainty estimation. In particular, for researchers in micro- and nano-measurement sciences where the governing laws of physics, chemistry, and biology are generally the objects of inquiry and thus not well-known for FEM implementation, the lack of a FEM simulation with uncertainty estimation is a major barrier. The development of a metrology-based mathematical modeling and simulation method such as the one presented here removes one of the barriers for enhancing the practice of fundamental science and engineering design through scientific computation and visualization. The DOE approach outlined in this paper not only answers the call of the 2006 NSF Blue Ribbon Panel Report on Simulation-Based Engineering Science⁵⁰ as quoted below:

" . . . verification, validation, and uncertainty quantification are challenging and necessary research areas that must be actively pursued,"

but also provides a tool for model verification as demanded by D. E. Post (Los Alamos National Laboratory) and L. G. Votta (Sun Microsystems) in a *Physics Today* (2005) article⁵¹:

" . . . New methods of verifying and validating complex codes are mandatory if computational science is to fulfill its promise for science and society."

Acknowledgment

We wish to thank Howard Baum, Ronald F. Boisvert, Robert F. Cook, Andrew Dienstfrey, Richard Fields, Richard Gates, Donna C. Hurley, Hung-kung Liu, Daniel Lozier, Geoffrey McFadden, Kuldeep Prasad, Ronald Rehm, Emil Simiu, Douglas Smith, Barry Taylor, and Nien-Fang Zhang, all of NIST, H. Norm Abramson of Southwest Research Institute, San Antonio, TX, Barry Bernstein of Illinois Inst. of Technology, Chicago, IL, Hal F. Brinson of University of Houston, Houston, TX, Michael Burger of LSTC Corp., Livermore, CA, Yuh J. (Bill) Chao of University of S. Carolina, Columbia, SC, Mel F. Kanninen of San Antonio, TX, Poh-Sang Lam of Savannah River National Laboratory, Aiken, SC, Bradley E. Layton of Drexel University, Philadelphia, PA, Pedro Marcal of MPave Corp., Julian, CA, Paul C. Mitiguy and Charles R. Steele of Stanford University, Stanford, CA, William Oberkampf and Jon Helton of Sandia National Laboratories, Albuquerque, NM, Robert Rainsberger of XYZ Scientific Applications, Inc., Livermore, CA, Glenn B. Sinclair of Louisiana State University, Baton Rouge, LA, Ala Tabiei of University of Cincinnati, Cincinnati, OH, and Tomasz Wierzbicki of M.I.T., Cambridge, MA, for their valuable discussions/comments during the course of this investigation.

The work reported here has been supported, in part, by NIST through three intramural grants over a span of four years, namely, (a) a 2003 contract award to the first author (Fong), P. O. No. NA1341-03-W-0536, entitled "Modeling and Analysis of Structural Integrity of a Complex Structure under Mechanical and Thermal Loading," (b) a 2004-05 competence award to the first two authors (Fong & Filliben) on "Complex System Failure Analysis: A Computational Science Approach," and (c) a 2005-06 exploratory competence award to three of the four authors (Fong, Filliben & deWit) on "A Stochastic Approach to Modeling of Contact Dynamics in Atomic Force Acoustic Microscopy," for which each of the individual awardees are grateful.

Disclaimer:

The views expressed in this paper are strictly those of the authors and do not necessarily reflect those of their affiliated institutions. The mention of the names of all commercial vendors and their products is intended to illustrate the capabilities of existing products, and should not be construed as endorsement by the authors or their affiliated institutions.

References

- [1] Filliben, J. J., and Heckert, N. A., 2002, *DATAPLOT: A Statistical Data Analysis Software System*, a public domain software released by NIST, Gaithersburg, MD 20899, <http://www.itl.nist.gov/div898/software/dataplot.html> (2002).
- [2] Hughes, T. J. R., *The Finite Element Method: Linear Static and Dynamic Finite Element Analysis*, revised edition of an original version published in 1987 by Prentice-Hall entitled "The Finite Element Method." Dover (2000).
- [3] Zienkiewicz, O. C., and Taylor, R. L., *The Finite Element Method*, 5th ed., Vol. 1, The Basis. Butterworth-Heinemann (2000).

- [4] ABAQUS, 2007, *ABAQUS User's Manual*, Version 6.7.0. ABAQUS, Inc., 1080 Main St., Pawtucket, Rhode Island 02860-4847 (2007).
- [5] ANSYS, 2007, *ANSYS User's Manual*, Release 10.0. ANSYS, Inc., 275 Technology Dr., Cannonsburg, PA 15317 (2006).
- [6] LSTC, 2003, *LS-DYNA Keyword User's Manual*, Version 970, April 2003, Livermore Software Technology Corp., Livermore, CA (2003).
- [7] Kwon, Y. W., and Bang, H. C., *The Finite Element Method Using MATLAB*, 2nd ed. CRC Press (2000).
- [8] Baker, N., Holst, M., and Wang, F., "Adaptive multilevel finite element solution of the Poisson-Boltzmann equation II: Refinement at solvent accessible surfaces in biomolecular systems," *J. Comput. Chem.*, Vol. 21, No. 15, pp. 1343-1352 (2000).
- [9] Gladilin, E., Micoulet, A., Hosseini, B., Rohr, K., Spatz, J., and Eils, R., "3D finite element analysis of uniaxial cell stretching: from image to insight," *Phys. Biol.*, Vol. 4, pp. 104-113 (2007).
- [10] Borodkin, J., and Hollister, S., "A New Method for Correcting Boundary Condition Errors on Microstructural FEA Models of Trabecular Bone and Implant Interfaces," in *Computer Methods in Biomechanics & Biomedical Engineering*, J. Middleton, M. L. Jones, and G. N. Pande, eds., pp. 105-114. Gordon and Breach (1996).
- [11] Kormi, K., Webb, D. C., and Tan, L. -B., "A Finite Element Simulation of Arterial Orifice Dilation by Angioplasty Balloon Insertion," in *Computer Methods in Biomechanics & Biomedical Engineering*, J. Middleton, M. L. Jones, and G. N. Pande, eds., pp. 305-314. Gordon and Breach (1996).
- [12] Bhattacharya, A. K., and Nix, W. D., "Analysis of Elastic and Plastic Deformation Associated with Indentation Testing of Thin Films on Substrates," *Int. J. Solids Struct.*, Vol. 24, No. 12, pp. 1287-1298 (1988).
- [13] Baker, N., Holst, M., et al, "Toward Computational Cell Biology: Nanostructures," *San Diego Supercomputer Center (SDSC) EnVision*, Vol. 16, No. 3, pp. 1-7 (2006).
<http://www.sdsc.edu/pub/envision/v16.3/baker.html>
- [14] Ayyub, B. M., ed., *Uncertainty Modeling and Analysis in Civil Engineering*. CRC Press (1998).
- [15] Lord, G. J., and Wright, L., "Uncertainty Evaluation in Continuous Modeling," Report to the National Measurement System Policy Unit, Department of Trade and Industry, NPL Report CMSC 31/03. Teddington, Middlesex, U.K.: National Physical Laboratory (2003).
- [16] Hlavacek, I., Chleboun, J., and Babuska, I., *Uncertain Input Data Problem and the Worst Scenario Method*. Elsevier (2004).
- [17] Oberkampf, W. L., "A Proposed Framework for Computational Fluid Dynamics Code Calibration/Validation," *Proc. 18th AIAA Aerospace Ground Testing Conference*, Colorado Spring, CO, AIAA Paper No. 94-2540 (1994).
- [18] Roache, P. J., *Verification and Validation in Computational Science and Engineering*. Hermosa Publishers, Albuquerque, NM (1998).
- [19] Oberkampf, W. L., Trucano, T. G., and Hirsch, C., "Verification, Validation, and Predicative Capability in Computational Engineering and Physics," *Proc. Workshop on Foundations for V & V in the 21st Century, 22-23 Oct. 2002*, John Hopkins Univ./Appl. Phys. Lab., Laurel, Maryland, D. Pace & S. Stevenson, eds., published by Society for Modeling & Simulation International (2002).

- [20] Babuska, I., and Oden, J. T., "Verification and validation in computational engineering and science: basic concepts," *Comput. Methods Appl. Mech. Engrg.*, Vol. 193, pp. 4057-4066 (2004).
- [21] Fong, J. T., "ABC of Statistics for Verification and Validation (V&V) of Simulations of High-Consequence Engineering Systems," *Proc. 2005 ASME Pressure Vessels and Piping Conference, July 17-21, 2005, Denver, CO*, Paper No. PVP2005-MF-13-1 (2005).
- [22] Butler, B. P., Cox, M. G., Forbes, A. B., Harris, P. M., and Lord, G. J., "Model Validation in the Context of Metrology: A Survey," *UK NMS Software Support for Metrology Programme, Model Validation Survey v1.0, NPL Report CISE 19/99*. Teddington, Middlesex, U.K.: National Physical Laboratory (1999).
- [23] Fong, J. T., Filliben, J. J., deWit, R., Fields, R. J., Bernstein, B., and Marcal, P. V., "Uncertainty in Finite Element Modeling and Failure Analysis: A Metrology-Based Approach," *ASME Trans., J. Press. Vess. Tech.*, Vol. 128, pp. 140-147 (2006).
- [24] Department of Defense (DOD), *DOD Directive No. 5000.61: Modeling and Simulation (M&S) Verification, Validation, and Accreditation (VV&A)*, Defense Modeling and Simulation Office, Office of the Director of Defense Research and Engineering (1996).
- [25] ANS, *Guidelines for the Verification and Validation of Scientific and Engineering Computer Programs for the Nuclear Industry*, American Nuclear Society, ANSI/ANS-10.4-1987 (1987).
- [26] AIAA, *Guide for the Verification and Validation of Computational Fluid Dynamics Simulations*, American Institute of Aeronautics and Astronautics, AIAA-G-077-1998, Reston, VA (1998).
- [27] ASME, *Guide for Verification and Validation in Computational Solid Mechanics*, American Society of Mechanical Engineers, ASME-PTC-60-Guide, V&V 10-2006, Product Catalog - Codes and Standards - Computational/Analysis., New York, NY (2006).
- [28] Cohen, M. L., Ralph, J. E., and Steffey, D. L., eds., 1998, *Statistics, Testing, and Defense Acquisition: New Approaches and Methodological Improvements*, National Academy Press, Washington, DC (1998).
- [29] Haldar, A., Guran, A., and Ayuub, B. M., eds. *Uncertainty Modeling in Finite Element, Fatigue and Stability of Systems*. World Scientific Publishing Co. Pte. Ltd., 1060 Main Street, River Edge, NJ 07661 (1997).
- [30] Haldar, A., and Mahadevan, S., *Reliability Assessment Using Stochastic Finite Element Analysis*. Wiley (2000).
- [31] Yang, D., Oh, S. L., Huh, H., and Kim, Y. H., eds., "Numisheet 2002: Design Innovation Through Virtual Manufacturing," *Proc. 5th Int. Conf. and Workshop on Numerical Simulation of 3D Sheet Forming Processes - Verification of Simulation and Experiment*, 21-25 October 2002, Jeju Island, Korea, Vol. 2, published by Korea Advanced Inst. of Science and Technology (KAIST), 373-1, Science Town, Taejon, 305-701, Korea (2002).
- [32] Fong, J. T., Filliben, J. J., deWit, R., and Bernstein, B., "Stochastic Finite Element Method (FEM) and Design of Experiments for Pressure Vessel and Piping (PVP) Decision Making," *Proc. of 2006 ASME Pressure Vessels and Piping Division Conference*, July 23-27, 2006, Vancouver, B. C., Canada, paper no. PVP2006-ICPVT11-93927. New York, NY: American Society of Mechanical Engineers (2006).
- [33] ISO, 1993, *Guide to the Expression of Uncertainty in Measurement*, prepared by ISO Technical advisory Group 4 (TAG 4), Working Group 3 (WG 3), Oct. 1993. ISO/TAG 4, sponsored by the BIPM (Bureau International des Poids et Mesures), IEC (International Electrotechnical Commission), IFCC (International Federation of Clinical Chemistry), ISO, IUPAC (Int. Union of Pure and Applied Chemistry), IUPAP (International Union of Pure and Applied Physics), and OIML (Int. Organization of Legal Metrology) (1993).

- [34] Taylor, B. N., and Kuyatt, C. E., *Guidelines for Evaluating and Expressing the Uncertainty of NIST Measurement Results*, NIST Tech. Note 1297, Sep. 1994 edition (supersedes Jan. 1993 edition), prepared under the auspices of the NIST Ad Hoc Committee on Uncertainty Statements, U. S. Government Printing Office, Washington, DC (1994).
- [35] Natrella, M. G., *Experimental Statistics*, NBS Handbook 91, 1963 edition (reprinted October 1966 with corrections). U. S. Government Printing Office, Washington, DC (1966).
- [36] John, P. W. M., *Statistical Design and Analysis of Experiments*, SIAM Classics in Applied Mathematics, Philadelphia, PA (1971).
- [37] Box, G. E., Hunter, W. G., and Hunter, J. S., 1978, *Statistics for Experimenters: An Introduction to Design, Data Analysis, and Model Building*. Wiley (1978).
- [38] Montgomery, D. C., *Design and Analysis of Experiments*, 5th ed. Wiley (2000).
- [39] Croarkin, C., Guthrie, W., Heckert, N. A., Filliben, J. J., Tobias, P., Prins, J., Zey, C., Hembree, B., and Trutna, eds., 2003, *NIST/SEMATECH e-Handbook of Statistical Methods, Chapter 5 on Process Improvement (pp. 1-480)*, <http://www.itl.nist.gov/div898/handbook/>, first issued, June 1, 2003, and last updated July 18, 2006. Produced jointly by the Statistical Engineering Division of the National Institute of Standards & Technology, Gaithersburg, MD, and the Statistical Methods Group of SEMITECH, Austin, TX. Also available as a NIST Interagency Report in a CD-ROM upon request to alan.heckert@nist.gov (2006).
- [40] Timoshenko, S., and Young, D. H., 1955, *Vibration Problems in Engineering*, 3rd ed. D. Van Nostrand (1955)
- [41] Clough, R., and Penzien, J., 2003, *Dynamics of Structures*, 2nd ed. (Revised). Berkeley, CA 94704: Computers and Structures, Inc. (2003).
- [42] Myers, R. H., and Montgomery, D. C., *Response Surface Methodology: Process and Product Optimization Using Designed Experiments*, 2nd ed. Wiley (2002).
- [43] Nelson, P. R., Coffin, M., and Copeland, K. A. F., *Introductory Statistics for Engineering Experimentation*. Elsevier (2003).
- [44] Liu, H. K., and Zhang, N. F., "Bayesian Approach to Combining Results from Multiple Methods," *Proc. Amer. Stat. Assoc.*, pp. 158-163 (2002).
- [45] Rabe, U., Janser, K., and Arnold, W., "Vibrations of free and surface-coupled atomic force microscope cantilevers: Theory and experiment," *Rev. Sci. Instrum.*, 67 (9), 3281-3293 (1996).
- [46] Kester, E., Rabe, U., Presmanes, L., Tailhades, Ph., and Arnold, W., "Measurement of Young's modulus of nanocrystalline ferrites with spinel structures by atomic force acoustic microscopy," *J. Phys. Chem. Solids*, 61, 1275-1284 (2000).
- [47] Hurley, D. C., Shen, K., Jennett, N. M., and Turner, J. A., "Atomic force acoustic microscopy methods to determine thin-film elastic properties," *J. Appl. Phys.*, 94(4), 2347-2354 (2003).
- [48] Lekhnitskii, S. G., *Theory of Elasticity of an Anisotropic Body*, translated from the revised 1977 Russian edition. Moscow: MIR Publishers (1981).
- [49] McSkimin, H. J., and Andreatch, P., Jr., "Elastic Moduli of Silicon vs. Hydrostatic Pressure at 25.0 C and - 195.8 C," *J. Appl. Phys.*, 35(7), 2161-2165 (1964).

- [50] Oden, J. T. (Chair), et al, 2006, "Simulation-Based Engineering Science (SBES): Revolutionizing Engineering Science through Simulation," Report of the NSF Blue Ribbon Panel on SBES, Feb. 2006 http://www.ices.utexas.edu/events/SBES_Final_Report.pdf
- [51] Post, D. E., and Votta, L. G., "Computational Science Demands a New Paradigm," Physics Today, Jan. 2005, pp. 35-41 (2005).